

Accepted Manuscript

Indole-3-carbinol (I3C) analogues are potent small molecule inhibitors of NEDD4-1 ubiquitin ligase activity that disrupt proliferation of human melanoma cells

Jeanne G. Quirit, Sergey N. Lavrenov, Kevin Poindexter, Janice Xu, Christine Kyauk, Kathleen A Durkin, Ida Aronchik, Thomas Tomasiak, Yaroslav A. Solomatin, Maria N. Preobrazhenskaya, Gary L. Firestone

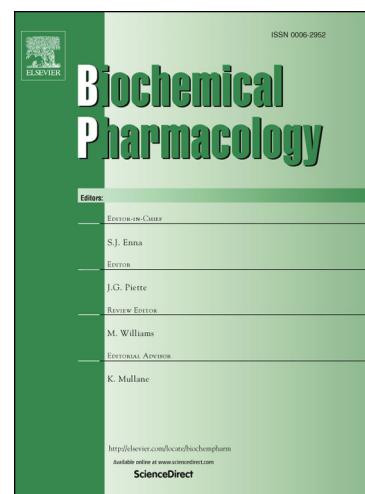
PII: S0006-2952(16)30469-5
DOI: <http://dx.doi.org/10.1016/j.bcp.2016.12.007>
Reference: BCP 12699

To appear in: *Biochemical Pharmacology*

Received Date: 30 August 2016
Accepted Date: 9 December 2016

Please cite this article as: J.G. Quirit, S.N. Lavrenov, K. Poindexter, J. Xu, C. Kyauk, K.A. Durkin, I. Aronchik, T. Tomasiak, Y.A. Solomatin, M.N. Preobrazhenskaya, G.L. Firestone, Indole-3-carbinol (I3C) analogues are potent small molecule inhibitors of NEDD4-1 ubiquitin ligase activity that disrupt proliferation of human melanoma cells, *Biochemical Pharmacology* (2016), doi: <http://dx.doi.org/10.1016/j.bcp.2016.12.007>

This is a PDF file of an unedited manuscript that has been accepted for publication. As a service to our customers we are providing this early version of the manuscript. The manuscript will undergo copyediting, typesetting, and review of the resulting proof before it is published in its final form. Please note that during the production process errors may be discovered which could affect the content, and all legal disclaimers that apply to the journal pertain.



**Indole-3-carbinol (I3C) analogues are potent small molecule inhibitors of NEDD4-1
ubiquitin ligase activity that disrupt proliferation of human melanoma cells**

Jeanne G. Quirit ^a, Sergey N. Lavrenov ^b, Kevin Poindexter ^a, Janice Xu ^a, Christine Kyauk ^a,
Kathleen A Durkin ^c, Ida Aronchik ^a, Thomas Tomasiak ^d, Yaroslav A. Solomatin ^b, Maria N.
Preobrazhenskaya ^b and Gary L. Firestone ^a *

^a Dept. of Molecular and Cell Biology and The Cancer Research Laboratory, University of
California at Berkeley, Berkeley, CA, USA, ^b Gause Institute of New Antibiotics, B.
Pirogovskaya 11, Moscow 119021, Russia, ^c Molecular Graphics and Computational Facility,
College of Chemistry, University of California, Berkeley, CA, USA; ^d Department of
Biochemistry and Biophysics, University of California, San Francisco, CA, USA

Email addresses of authors: Jeanne Quirit, jgquirit@berkeley.edu; Sergey Lavrenov,
satory@mail.ru; Kevin Poindexter, kpoindexter25@gmail.com; Janice Xu,
jamicexu@scripps.edu; Christine Kyauk, ckyauk@berkeley.edu; Kathleen Durkin,
durkin@berkeley.edu; Ida Aronchik, idaaronchik@gmail.com; Thomas Tomasiak,
tomasiak@msg.ucsf.edu; Yaroslav Solmatin, hercules44@yandex.ru; Maria Preobrazhenskaya,
satory@mail.ru; Gary Firestone, glfire@berkeley.edu.

Corresponding author: Gary L. Firestone, Dept. of Molecular and Cell Biology, 591 LSA, Univ.
California at Berkeley, Berkeley, CA 94720-3200; email: glfire@berkeley.edu, Phone: (510)
642-8319.

Abstract

The HECT domain-containing E3 ubiquitin ligase NEDD4-1 (Neural precursor cell Expressed Developmentally Down regulated gene 4-1) is frequently overexpressed in human cancers and displays oncogenic-like properties through the ubiquitin-dependent regulation of multiple protein substrates. However, little is known about small molecule enzymatic inhibitors of HECT domain-containing ubiquitin ligases. We now demonstrate that indole-3-carbinol (I3C), a natural anti-cancer phytochemical derived from cruciferous vegetables such as cabbage and broccoli, represents a new chemical scaffold of small molecule enzymatic inhibitors of NEDD4-1. Using *in vitro* ubiquitination assays, I3C, its stable synthetic derivative 1-benzyl-I3C and five novel synthetic analogues were shown to directly inhibit NEDD4-1 ubiquitination activity. Compared to I3C, which has an IC₅₀ of 284 μ M, 1-benzyl-I3C was a significantly more potent NEDD4-1 enzymatic inhibitor with an IC₅₀ of 12.3 μ M. Compounds 2242 and 2243, the two indolecarbinol analogues with added methyl groups that results in a more nucleophilic benzene ring π system, further enhanced potency with IC₅₀s of 2.71 μ M and 7.59 μ M, respectively. Protein thermal shift assays that assess small ligand binding, in combination with *in silico* binding simulations with the crystallographic structure of NEDD4-1, showed that each of the indolecarbinol compounds bind to the purified catalytic HECT domain of NEDD4-1. The indolecarbinol compounds inhibited human melanoma cell proliferation in a manner that generally correlated with their effectiveness as NEDD4-1 enzymatic inhibitors. Taken together, we propose that I3C analogues represent a novel set of anti-cancer compounds for treatment of human melanomas and other cancers that express indolecarbinol-sensitive target enzymes.

Key Words:

Indole-3-carbinol analogues

Ligand-target protein interactions

NEDD4-1 ubiquitin ligase

In silico computational modeling

Anti-cancer compounds

Melanoma cells

1. Introduction

E3 ubiquitin ligases play critical roles in controlling numerous cellular pathways by catalyzing the attachment of ubiquitin protein chains to specific lysine residues of protein substrates that selectively signal protein degradation, localization, endocytosis, subcellular trafficking and/or activity. The diversity and number of the ubiquitination products determine the outcomes for individual protein substrates [1]. Of the several hundred known E3 ubiquitin ligases, approximately 30 have a distinguishing HECT (Homologous to E6-AP C-Terminus) domain in their structure that includes the catalytic site for ubiquitin protein ligation [2]. The NEDD4-1 (Neural precursor cell Expressed Developmentally Down regulated gene 4-1) ubiquitin ligase is one of nine members of the NEDD4 gene family of HECT domain-containing E3 ubiquitin ligases [3]. The structure of NEDD4-1 includes an N-terminal C2 calcium-dependent lipid binding domain involved in membrane interactions, a central domain that direct protein-protein interactions through several WW (double tyrosine residue) motifs and the C-terminal catalytic HECT domain [4]. NEDD4-1 is frequently overexpressed in different types of human cancers [5] and can exert effects on the development, progression, survival and proliferation of human cancers [5] through ubiquitination of a variety of downstream protein substrates including those linked to growth factor receptor signaling and tumor suppressor activities [6]. Based on these observations, the targeting NEDD4-1 has been proposed as a potential therapeutic strategy for treatment of human cancers [5], however, to date relatively little is known about small molecule enzymatic inhibitors of NEDD4-1 or any other HECT domain containing E3 ubiquitin ligases.

We have been investigating the anti-cancer properties of indole-3-carbinol (I3C), which is derived by hydrolysis from glyco Brassica produced in cruciferous vegetables of the *Brassica* genus such as cabbage, broccoli and Brussels sprouts. I3C is a natural indolecarbinol phytochemical that can activate multiple anti-proliferative cascades in several types of human cancers, including melanoma, breast, prostate, lung, colon, leukemia, and cervical cancer [7-17]. The cellular pathways under I3C control involve transcriptional, enzymatic, metabolic and cell signaling processes that can lead to an arrest of cell cycle progression, apoptosis, loss of cell survival signaling, down-regulation of cancer cell migration, modulation of hormone receptor signaling, and inhibition of tumor growth [18-30]. A key advance in understanding the I3C anti-proliferative mechanism is our discovery that I3C triggers distinct and overlapping sets of anti-proliferative signaling events by direct interactions with specific target proteins [31-34]. The serine protease elastase was the first identified I3C target protein, with I3C functioning as a direct noncompetitive inhibitor of elastase enzymatic activity [31]. In human breast cancer cells, cell surface-associated elastase cleaves the CD40 member of the tumor necrosis factor receptor to stimulate a pro-proliferative cascade resulting in the activation of the NFkB [35-38]. The I3C inhibition of elastase activity prevents CD40 cleavage and shifts the down stream signaling in a manner that disrupts NFkB-dependent cell cycle and proliferative gene expression [32]. These observations suggest that I3C may mediate its anti-proliferative effects in other types of cancer cells by directly interacting with other classes of target proteins with enzymatic activities.

We recently documented that I3C arrests the proliferation and induces apoptosis of human melanoma cells [34, 39]. The most sensitive melanoma cells expressed an oncogenic form of BRAF and the wild type PTEN (phosphatase and tensin homologue detected on chromosome 10),

which is a lipid phosphatase that acts a tumor suppressor protein [40-42]. Concomitant with the proliferative arrest, I3C down-regulated the NEDD4-1 mediated ubiquitination of wild type PTEN, which resulted in higher levels of this tumor suppressor protein [34]. Furthermore, siRNA knock down of NEDD4-1 mimicked the I3C stabilization of PTEN protein and isothermal titration calorimetry demonstrated that I3C directly binds to the purified HECT catalytic domain of NEDD4-1 [34]. Taken together, these observations suggest the possibility that I3C may act as a direct inhibitor of NEDD4-1 ubiquitin ligase activity.

In silico binding simulations between I3C and the crystallographic structure of NEDD4-1, using shape and electrostatics as restrictive parameters, predicted that I3C binds to a small subdomain of the N-lobe of the catalytic HECT domain, but not to the C2 and WW domains [34]. These modeling results suggest that I3C could provide a chemical starting point to develop highly potent anti-cancer compounds based on enhanced target protein interactions. 1-benzyl-indole-3-carbinol (1-benzyl-I3C), which has a benzyl moiety attached to the indole ring nitrogen, was synthesized and shown to have a more potent anti-proliferative response in human breast cancer cells compared to I3C and is a more potent elastase inhibitor [33]. The enhanced efficacy of 1-benzyl-I3C is due to significantly increased hydrophobic character and greater stability compared to I3C due to the steric effect of the bulky 1-benzyl substituent that hampers oligomerization of the 1-benzyl-indol-3-yl methyl cation [32]. We now demonstrate that I3C represents a chemical scaffold to develop highly potent small molecule inhibitors of NEDD4-1 ubiquitin ligase activity. Furthermore, we show that the indolecarbinol compounds bind to NEDD4-1 and robustly inhibit the proliferation of human melanoma cells with efficacies that generally correlated with their effectiveness in inhibiting NEDD4-1 activity, which implicates

their potential use as a novel set of anti-cancer compounds for treatment of human melanomas and other cancers.

2. Materials and Methods

2.1 Synthesis and characterization of I3C analogues LCTA-2160, LCTA-2242, LCTA-2243, LCTA-2244 and LCTA-2163

2.1.1. General information

NMR spectra were registered on a Varian VXR-400 instrument operated at 400 MHz (^1H NMR). TLC was performed on Silica Gel F254 plates (Merck) uses systems A (petroleum ether), B (petroleum ether-ethyl acetate 10:1) and C (petroleum ether-ethyl acetate 1:1). Column chromatography was performed on Silica Gel Merck 60. Melting points were determined on a Buchi SMP-20 apparatus and are uncorrected. High-resolution mass spectra were recorded with electron-spray ionization on a Bruker Daltonics microOTOF-QII instrument. HPLC was performed using Shimadzu LC-20AD (Japan), column Kromasil (Sweden) 100-C18, size 5mm, 4.6x250 mm, loop 20mk1, elution: (I) $\text{H}_2\text{O} \rightarrow \text{CH}_3\text{CN}$ gradient from 10% to 95% CH_3CN at 20 min. (II)- H_3PO_4 0.01 M in water $\rightarrow \text{CH}_3\text{CN}$ gradient from 10% to 95% CH_3CN at 20 min. All solutions were dried over Na_2SO_4 and evaporated at reduced pressure on a Buchi-R200 rotary evaporator at the temperature below 35° C. All products were vacuum dried at room temperature. All solvents, chemicals and reagents were obtained commercially from SigmaAldrich or Merck and used without purifications.

2.1.1.2. Compounds **3** (LCTA-2160; LCTA-2242; LCTA-2243; LCTA-2244) were synthesized by Scheme 1 (Fig.1A). Compound LCTA-2163 was prepared by Scheme 2 starting from 2-(thiophen-2-yl)-indole (Fig.1B).

2.1.1.3. 1-Phenyl-*1H*-indole (**3a**). As previously described [43], for N-phenylation of indoles a mixture of indole **1** (0.585 g, 5 mmol), iodobenzene **2a** (1.26 g, 6.2 mmol), K₂CO₃ (1.38 g, 10 mmol), L-proline (0.23 g, 2 mmol), CuI (0.19 g, 1 mmol) in 20 ml of DMSO was heated at 130°C for 3h. The cooled mixture was diluted by water (100 ml) and extracted by diethyl ether (30 ml). Organic layer was separated, washed by brine, dried over Na₂SO₄ and concentrated in vacuo. The residual oil was loaded on a silica gel column and eluted with petroleum ether to afford the **3a** (0.48 g, 50% yield) as yellow oil. R_f 0.27 (A)

2.1.1.4. The compounds **3b**, **3c**, **3d** were similarly prepared from indole and the appropriated iodarenes : 1-*p*-Tolyl-*1H*-indole (**3b**), 40% yield, yellow oil, R_f 0.33 (A) ; 1-*o*-Tolyl-*1H*-indole (**3c**), 50% yield, yellow oil, R_f 0.33 (A); 1-(3,4-Dimethoxyphenyl)-*1H*-indole (**3d**), 48% yield, yellow oil, R_f 0.15 (A).

2.1.1.5. 1-Benzyl-2-(thiophen-2-yl)-*1H*-indole (**3e**). To a stirred solution of 2-(thiophen-2-yl)-*1H*-indole (**1e**) (prepared by cyclization of 2-acetylthiophene phenylhydrazone as previously described [44]) (1g, 5 mmol) in DMSO (30 ml) finely ground KOH (0.84 g, 15 mmol) was added. After 30 min incubation benzyl bromide (**2e**) (1g, 6 mmol) was added and reaction mixture allowed to stir at 20°C for 12 h. After that mixture was diluted by water (100 ml) and extracted by diethyl ether (30 ml). Organic layer was separated, washed by brine, dried over Na₂SO₄ and

concentrated in vacuo. The residual oil was loaded on a silica gel column and eluted with petroleum ether to afford the **3e** (1.15 g, 80% yield) as yellow oil.

2.1.1.6. 1-Phenyl-*1H*-indole-3-carbaldehyde (**4a**). To a stirred solution of **3a** (0.48 g, 2.5 mmol) in 20 ml DMF at 0°C was added dropwise POCl₃ (0.46 g, 3 mmol). After complete addition the temp was increased to 20°C and kept at this temp for 12 h. The solution was diluted by water (200 ml) and extracted by diethyl ether (50 ml). Aqueous layer was separated and treated by 5N NaOH to pH 10. The oil emulsion obtained was extracted by diethyl ether (50 ml), washed by brine, dried over Na₂SO₄, concentrated in vacuo and crystallized from methanol to produce **4a** as colorless crystals (0.41 g, 75% yield), Mp 70-72°C, R_f 0.61 (B).

2.1.1.7. The compounds **4b-e** were similarly prepared from the appropriated indoles **3**: 1-*p*-Tolyl-*1H*-indole-3-carbaldehyde (**4b**), 80% yield; colorless crystals, Mp 112-115°C, R_f 0.65 (B); 1-*o*-Tolyl-*1H*-indole-3-carbaldehyde (**4c**), 65% yield, colorless crystals, Mp 74-76°C, R_f 0.65 (B); 1-(3,4-Dimethoxyphenyl)-*1H*-indole-3-carbaldehyde (**4d**), 60% yield, colorless crystals, Mp 122-124°C, R_f 0.44 (B); 1-Benzyl-2-(thiophen-2-yl)-*1H*-indole-3-carbaldehyde (**4e**), 60% yield; yellow crystals, Mp 205-207°C, R_f 0.62 (B)

2.1.1.8. (1-Phenyl-*1H*-indol-3-yl)methanol (**5a**) **LCTA-2160**. NaBH₄ (0.1 g, 2.7 mmol) was added to solution of **4a** (0.41 g; 1.8 mmol) in ethanol (25 mL) and stirred for 2 h at room temperature. The solvent was removed in vacuo at the temperature below 25°C, the residue obtained was solved in water (100 mL) and the solution was extracted with diethyl ether (3 × 20

mL). The combined organic phases were washed by brine, dried over Na₂SO₄ and concentrated in vacuo at the temperature below 25°C to produce **5a** as colorless oil (0.28 g, 70% yield).

δ (ppm) [DMSO-d₆]: 4.70 (2H, d, J 4Hz, 3-CH₂), 4.92 (1H, t, J 4Hz, OH), 7.14 (2H, m, H-5,6), 7.40 (7H, m, H-2, 4, 2', 3',4',5',6'), 7.69 (1H, d, J 8Hz, H-7). HRMS [M+Na]⁺, found 246.0865, [C₁₅H₁₃NO+Na]⁺ requires 246,0895. HPLC: (I) Rt 10.51 min, purity 96%. R_f 0.65 (C).

2.1.1.9. The compounds **5 b-e** were similarly prepared from the appropriated indole-3-carbaldehydes **4**: (1-*p*-Tolyl-1*H*-indol-3-yl)methanol (**5b**), yield 70%, colorless crystals, Mp 72-75°C. δ (ppm) [DMSO-d₆]: 2.37 (3H, s, Ar-CH₃), 4.71 (2H, d, J 4Hz, 3-CH₂), 4.94 (1H, t, J 4Hz, OH), 7.16 (2H, m, H-5,6), 7.41 (6H, m, H-2, 4, 2', 3',5',6'), 7.71 (1H, d, J 8Hz, H-7). HRMS [M+Na]⁺, found 260.1020, [C₁₆H₁₅NO+Na]⁺ requires 260,1051. HPLC: (II) Rt 12.78 min, purity 99%. R_f 0.58 (C).

2.1.1.10 (1-*o*-Tolyl-1*H*-indol-3-yl)methanol (**5c**): yield 65%, colorless crystals, Mp 43-45°C. δ (ppm) [DMSO-d₆]: 2.01 (3H, s, Ar-CH₃), 4.72 (2H, d, J 4Hz, 3-CH₂), 4.95 (1H, t, J 4Hz, OH), 6.91 (1H, d, J 8Hz, H-4), 7.10 (2H, m, H-5,6), 7.36 (5H, m, H-2, 3',4',5',6'), 7.72 (1H, d, J 4Hz, H-7). HRMS [M+Na]⁺, found 260.1024, [C₁₆H₁₅NO+Na]⁺ requires 260,1051. HPLC: (II) Rt 12.03 min, purity 95%. R_f 0.60 (C).

2.1.1.11 (1-(3,4-Dimethoxyphenyl)-1*H*-indol-3-yl)methanol (**5d**): yield 65%, colorless crystals, Mp 96-98°C. δ (ppm) [DMSO-d₆]: 3.72 (3H, s, OCH₃), 3.84 (3H, s, OCH₃), 4.68 (2H, d, J 4Hz, 3-CH₂), 4.90 (1H, t, J 4Hz, OH), 6.65 (1H, d, J 12Hz, 5'-H), 6.80 (1H,s, H-2'), 6.98 (1H, d,

J 8Hz, H-4), 7.07 (2H, m, H-5,6), 7.24 (2H,m, H-2,6'). HRMS $[M+Na]^+$, found 306.1084, $[C_{17}H_{17}NO_3+Na]^+$ requires 306,1106. HPLC: (II) Rt 10.06 min, purity 99%. R_f 0.44 (C).

2.1.1.12 (1-Benzyl-2-(thiophen-2-yl)-1*H*-indol-3-yl)methanol (**5e**): yield 60%, brownish oil. δ (ppm) [DMSO- d_6]: 4.60 (2H, d, J 8Hz, 3-CH₂), 4.85 (1H, t, J 8Hz, OH), 5.42 (2H, s, CH₂-Ph), 6.90 (1H, d, J 8Hz, H-4), 7.23 (10H, m, H-5,6 of indole, 2-5 of Ph and 3-5 of thiophene), 7.74 (1H, d, J 8Hz, H-7). HRMS $[M+Na]^+$, found 342.0946, $[C_{17}H_{17}NO_3+Na]^+$ requires 342.0923. HPLC: (I) Rt 15.28 min, purity 95%. R_f 0.66 (C).

2.2. Biochemical Studies

2.2.1. In Vitro Protein Thermal Shift Assays

All reactions were set up in 20 μ L reactions in 96 well plates with total human NEDD4-1^{Hect} protein concentrations of 2.5 μ M and 10x SYPRO orange dye (ThermoFisher Scientific, Waltham, MA) [45]. The NEDD4-1 HECT domain was pre-incubated for 5 minutes with either I3C, 2244, 2160, or 2163 at 250 μ M while concentrations of 25 μ M was used for compounds 1-benzyl-I3C, 2242, and 2243. Thermal melting experiments were performed on the Viia7 instrument (Life Technologies, Foster City, CA) melt curve program with a heat ramp rate of 0.05°C/s and a temperature range beginning at 25°C and ending at 95°C. Melting temperatures were analyzed with Protein Thermal Shift Software (Life Technologies, Foster City, CA) to identify the midpoint of the transition with an analysis of the first derivative. All experiments were performed in triplicates.

2.2.2. In Vitro NEDD4-1 Enzymatic Assays

Purified NEDD4-1 protein and the indicated concentrations of indolecarbinol compounds were pre-incubated for 1 hour. The reaction mixtures were then transferred to an ELISA microplate where the remaining components of the ubiquitination reaction (E1, E2, and ubiquitin) were added. This plate captures poly-ubiquitin chains formed in an E3-dependent reaction and was initiated with ATP at room temperature for 1 hour. The plates were washed 3 times and incubated with biotin-linked ubiquitin antibody and was subsequently incubated with streptavidin-HRP. The E3LITE Customizable Ubiquitin Ligase Kit from LifeSensors (Malvern, PA) (Catalog #: UC101) is an ELISA-like highly sensitive assay that relies on enhanced chemiluminescence to quantitatively measure ubiquitin E2 conjugation and E3 ligase activity. No additional non-native tagging or labeling of ubiquitin was required. The assay is based on the ability of an ubiquitin-binding domain to preferentially bind polyubiquitin relative to monoubiquitin, thus measuring activity of E3 ligase that builds ubiquitin chains in a dose-dependent manner [53-56].

2.2.3. Statistical analysis

GraphPad Prism 6.0 software (GraphPad Software Inc., San Diego, CA, USA) was used to perform data analysis in all experiments. Data are presented as mean \pm SD from 3 independent experiments. Statistical analysis comparing the ubiquitin ligase activity for no added NEDD4-1 and untreated NEDD4-1 was analyzed by an unpaired t-test. Significance was assigned at a * p value $< \leq 0.05$; ** $p < 0.01$; *** $p < 0.001$.

2.3. Biological Studies

2.3.1 Melanoma and breast cancer cell culture and proliferation assays

The human G-361 melanoma and human MCF-7 breast cancer cell lines were purchased from American Type Culture Collection (ATCC) (Manassas, VA), and were authenticated according to the ATCC guidelines. Cells were cultured in Modified McCoy's 5A cell media supplemented with 10% fetal bovine serum (Gemini Bio Products, West Sacramento, CA), 2 mM L-glutamine, and 2.5 ml of 10,000 U/ml penicillin/streptomycin mixture (Gibco, Life Technologies, Carlsbad, CA). Melanoma and breast cancer cells were seeded on a 48-well plate in triplicates and upon 80-90% confluency were treated with I3C, 1-benzyl-I3C and the 1-benzyl-I3C analogues for 48 hours. Subsequently, inhibition of proliferation was assessed using the Dojindo Cell counting Kit -8 as per the protocol in the user's manual. Briefly, 50 μ l of the CCK-8 solution was added to each well along with 450 μ l media and incubated for 2-3 hours. The absorbance was read at 450nm and % inhibition was calculated for each condition standardizing DMSO to zero.

2.3.2. Western blot analysis

Western Blot analyses of samples electrophoretically fractionated on 8-10% acrylamide gels were carried out as previously described [32, 33]. ECL Lightening reagents were used to visualize the primary antibody bound protein bands in nitrocellulose membranes and the results captured on ECL Autoradiography Film (GE Healthcare, Piscataway, NJ). The western blots employed the following primary antibodies: MITF-M Monoclonal antibody (C5 Clone that recognizes the N-terminal fragment of human MITF protein as the immunogen, Thermo-Scientific, Waltham, MA), phospho-AKT-1 and total Akt-1 (Cell Signaling Technology, Danvers, MA), HSP 90 (BD Bio-sciences, San Jose, CA), Actin (Cytoskeleton Inc., Denver, CO). In cells treated with increasing concentrations of compound 2242, the relative levels of phosphorylated Akt-1 protein compared to the levels of total Akt-1 protein was quantified by

densitometry of the western blots. Densitometry was performed using ImageJ software (NIH, Bethesda, MD) and the results shown as relative densitometry units compared to untreated cells.

2.4. *In Silico* Computational Methods

2.4.1. *Protein Structure Preparation*

The coordinates for the NEDD4-1 HECT domain protein structure were obtained from the RCSB Protein Data Bank (PDB). 5C91 [46] was used to examine the interactions between the NEDD4-1 HECT domain and indolecarbinol compounds. The protein structure was prepared using the Schrödinger's Protein Preparation Wizard module (Schrödinger Suite 2015-4 Protein Preparation Wizard; Epik version 3.4, Schrödinger, LLC, New York, NY, 2015; Impact version 6.9, Schrödinger, LLC, New York, NY, 2015; Prime version 4.2, Schrödinger, LLC, New York, NY, 2015.) [47]. Hydrogen atoms were added and the side chain structures of Gln and Asn were flipped in order to yield the maximum degree of hydrogen bond interactions. The protein was subsequently minimized using the OPLS force field in the MacroModel module in Schrödinger (MacroModel, version 11.0, Schrödinger, LLC, New York, NY, 2015.) with backbone atoms fixed.

2.4.2. *Induced fit docking methods*

The NEDD4-1 HECT domain protein structure (PDB accession number: 5C91) was applied with the induced-fit docking (IFD) method in the Schrödinger software suite (Small-Molecule Drug Discovery Suite 2015-4: Schrödinger Suite 2015-4 Induced Fit Docking protocol; Glide version 6.9, Schrödinger, LLC, New York, NY, 2015; Prime version 4.2, Schrödinger, LLC, New York, NY, 2015) [48-50]. I3C, 1-benzyl-I3C, and their corresponding analogs were prepared using LigPrep (version 3.6, Schrödinger, LLC, New York, NY, 2015) and were optimized with the OPLS force

field in the MacroModel module in Schrödinger. Ligands were docked to the rigid protein using the soft-potential docking in the Glide program with the van der Waals radii scaling of 0.5 for the protein. The resulting top 20 poses of ligands were used to sample the protein plasticity using the Prime program (version 4.2, Schrödinger, LLC, New York, NY, 2015) in the Schrödinger suite [51, 52]. Flexibility of the protein was taken under consideration by having residues that were at least one atom within 5 Å of any of the 20 ligand poses subjected to a conformational search and minimization. Residues outside the zone were fixed. The new 20 protein conformations were subsequently utilized for redocking. In the final stage, the ligand poses were redocked using Glide SP into structures within 30.0 kcal/mol of the top 20 structures. The binding affinity of each complex was reported in the GlideScore. A more negative GlideScore is indicative of a more favorable binding interaction. Figures were made using the Pymol program (The PyMOL Molecular Graphics System, Version 1.8 Schrödinger, LLC.)

3. Results

3.1 *In silico* computational modeling of molecular interactions and direct binding of I3C and 1-Benzyl-I3C to the HECT domain of the ubiquitin ligase NEDD4-1

The natural compound I3C and its highly potent synthetic derivative 1-benzyl-I3C [33, 57], which has a benzyl moiety attached to the indole ring nitrogen, were initially used to assess the potential interactions of indolecarbinol compounds and their effects on the enzymatic activity of NEDD4-1, a HECT domain-containing ubiquitin ligase [58]. *In silico* molecular binding simulations using the Schrödinger Induced Fit Docking protocol were performed to evaluate and compare potential predicted binding sites within NEDD4-1^{HECT} for I3C and 1-benzyl-I3C.

Proteins recognize ligands based on 3D structure and electrostatic complementarities, and the Induced Fit Docking protocol was implemented for binding simulations because this program incorporates protein flexibility within a tested ligand-protein complex to account for the dependence of active site geometry upon conformational changes generated by a bound ligand. The previously reported structure of NEDD4-1^{HECT} co-crystalized with an indole-based small molecule (PDB ID: 5C91) [46] was used as the foundation structure for docking I3C or 1-benzyl-I3C to NEDD4-1^{HECT}. Predicted interactions with specific amino acid residues of the NEDD4-1^{HECT} domain are within 4 Å of either I3C or 1-benzyl-I3C.

Structural analysis shows that the NEDD4-1^{HECT} domain is a bi-lobed domain consisting of an N-terminal N-lobe that interacts with the E2 ubiquitin ligase and a C-terminal C lobe containing the catalytic cysteine and which is free to rotate around the flexible hinge that tethers it to the N lobe [58]. As shown in Figure 2A, computer modeling predicts that the hydrophobic indole core of I3C is oriented toward a pocket of the N-lobe and is enveloped by residues Tyr 634, Tyr 605, Leu 607, Asn 628, His 631, Cys 627 and Leu 553. In particular, the indole moiety of I3C is predicted to make aromatic edge-to-face interactions with residues Tyr 605 and Tyr 634 (Fig. 2A). Notably, Tyr 605 is an essential residue for noncovalent ubiquitin binding and poly-ubiquitination chain elongation by NEDD4-1 [46, 58]. Similarly to I3C, the indole moiety in 1-benzyl-I3C makes edge-to-face interactions with residues Tyr 605 and Tyr 634 and is securely positioned against residues Leu 553 and Glu 554. The additional phenyl moiety points toward a complementary cavity formed by Leu 607, His 631, Ser 624, Cys 627, Asn 628, and Asp 630 which may act to further stabilize and enhance 1-benzyl-I3C interactions with NEDD4-1 (Fig. 2B).

Protein Thermal Shift assays was used to directly test whether I3C and 1-benzyl-I3C can bind to the purified bacterially-synthesized HECT Domain of NEDD4-1 (NEDD4-1^{HECT}). Indolecarbinol-mediated alterations in thermostability of NEDD4-1^{HECT} are indicative of direct interactions between each potential ligand and the protein. Purified NEDD4-1^{HECT} at a concentration of 2.5 μM was incubated with 250 μM I3C, 25 μM 1-benzyl-I3C or with the vehicle control and each mixture was then treated with Sypro orange dye, which binds to hydrophobic regions of proteins and emits a fluorescent signal as the protein unfolds [45]. A 10-fold lower concentrations of 1-benzyl-I3C compared to I3C was used because this I3C derivative was previously shown to be significantly more potent than I3C in its ability to interact with human neutrophil elastase [33, 57]. The binding reactions were slowly heated from 25°C to 95°C, and the unfolding of the HECT domains continuously recorded from the fluorescent signals. Conditions that thermally stabilize the protein will typically shift the melting temperature upwards by 4° C to greater than 20° C. Generally as an empirical estimate, a greater than 4° C shift in melting temperature corresponds to binding of a ligand with a K_d of approximately $<1 \mu\text{M}$ [59], although the magnitude of the temperature shift does not necessarily correlate with ligand affinity. This assay was used to assess whether each indolecarbinol analogue binds directly to NEDD4-1, but was not employed to obtain more precise K_D values for each compound. As shown in Figure 2C, in the absence of added indolecarbinol compounds, the first derivative NEDD4-1^{HECT} melting profile yielded an apparent T_m of 48°C. Exposure to 250 μM I3C or 25 μM 1-benzyl-I3C stabilized the NEDD4-1^{HECT} secondary structure based on concomitant increases in melting temperatures or ΔT_m values of 13.3 °C for I3C and 10.2 °C for

1-benzyl-I3C. These results demonstrate that both indolecarbinol compounds directly bind to NEDD4-1^{HECT}.

3.2 I3C and enhanced potency 1-benzyl-I3C represent a new class of enzymatic inhibitors of NEDD4-1 ubiquitination Activity

Because the HECT domain of NEDD4-1 contains the catalytic site that mediates the ubiquitin ligase activity of this enzyme, the predicted locations of the *in silico* defined interaction sites of I3C and 1-benzyl-I3C and the fact that both indolecarbinol compounds directly bind to the HECT domain suggested the possibility that these indolecarbinol compounds could alter NEDD4-1 enzymatic activity. Relatively little is known about small molecular inhibitors of this important ubiquitin ligase. Therefore, an *in vitro* polyubiquitylation assay was optimized to test the potential effects and efficacy of I3C and 1-benzyl-I3C on NEDD4-1 activity. In order to validate and standardize the assay, ubiquitin ligase activity was initially monitored in the absence or presence of 20 ng of NEDD4-1, which is an E3 ubiquitin ligase. The reaction mixtures were then transferred to an ELISA microplate where the remaining contents of the reaction (E1, E2, and ubiquitin) were added. The plate captures poly-ubiquitin chains formed in an E3-dependent reaction and was initiated with ATP at room temperature for 1 hour. The washed plates were incubated with biotin-linked ubiquitin antibody and then incubated with streptavidin-HRP to monitor NEDD4-1 auto-ubiquitylation as the readout for NEDD4-1 activity. As shown in Figure 2D, no auto-ubiquitination activity was observed in the absence of NEDD4-1 whereas in the presence of 20 ng NEDD4-1, ubiquitin ligase activity was high at a relative rate of approximately 1.02 RFU/min confirming the functionality of the assay.

To directly determine the potential effects of indolecarbinol compounds on NEDD4-1 ubiquitin ligase activity, a range of concentrations of either I3C or 1-benzyl-I3C were tested in the *in vitro* polyubiquitylation assay in comparison to the biologically inactive I3C analog, tryptophol, which contains an ethanol group attached to the C3 ring carbon instead of a hydroxy methyl group and acts as a negative control. The reaction mixtures were preincubated with purified human NEDD4-1 protein for 1 hour and the formation of poly-ubiquitin chains was analyzed in an ELISA microplate in the presence of an E1 ligase, an E2 ligase and ubiquitin and the enzymatic reactions were initiated with ATP. The washed plates were first incubated with biotin-linked ubiquitin antibody and then incubated with streptavidin-HRP to monitor NEDD4-1 auto-ubiquitination as the readout for NEDD4-1 activity. As shown in Figure 2E, a high concentration of tryptophol had no effect on NEDD4-1 auto-ubiquitination activity, whereas I3C inhibited NEDD4-1 ubiquitin ligase activity with a half maximal inhibition IC_{50} of 284 μ M. In comparison to the natural indolecarbinol I3C, 1-benzyl-I3C displayed significantly more potent *in vitro* inhibitory effects on NEDD4-1 ubiquitin ligase activity with an IC_{50} of 12.3 μ M, which represents an approximate 23-fold higher efficacy than I3C (Fig. 2E). These results establish I3C and the highly potent 1-benzyl-I3C as small molecule inhibitors of NEDD4-1 enzymatic activity and further implicate indolecarbinol compounds as a novel class of inhibitors of HECT-domain ubiquitin ligases.

3.3 Anti-proliferative responsiveness of I3C and 1-Benzyl-I3C in human G361 melanoma cells

Before analyzing the effects of an expanded set of indolecarbinol derivatives on NEDD4-1, it was important to determine whether the differences in effectiveness of I3C and 1-benzyl-I3C to inhibit NEDD4-1 enzymatic activity generally reflected the relative efficacies of these

indolecarbinol compounds on anti-proliferative responses in melanoma cells. The Microphthalmia Associated Transcription Factor isoform M (MITF-M), a basic helix-loop-helix leucine zipper transcription factor, is highly involved with melanoma cell proliferation, cell cycle control and cell survival through its transcriptionally regulated gene products [60-62]. We recently observed that I3C down regulates MITF-M expression by disruption of oncogenic BRAF signaling through the Brn2 transcriptional regulator of MITF-M [39]. Therefore, human G361 melanoma cells, which display an oncogenic BRAF/wild type PTEN genotype and are highly sensitive to the anti-proliferative effects of I3C, were treated with a range of concentrations of either I3C or 1-benzyl-I3C for 48 hours and the MITF-M protein levels determined by western blot analysis. As shown in Figure 3A (left panel), I3C and 1-benzyl-I3C strongly down regulated MITF-M protein levels. MITF-M protein appears as a doublet band in 1-benzyl-I3C treated cells, although the underlying mechanism is not known. Importantly, quantification of the relative levels of MITF-M protein by densitometry compared to the HSP90 demonstrated that 1-benzyl-I3C displayed significantly enhanced efficacy compared to I3C (Fig 3A, right panel).

MITF-M induces expression of several G1 acting cell cycle genes [63, 64], such as CDK4, CDK2 and cyclin D1, suggesting that the I3C and 1-benzyl-I3C-mediated loss of MITF-M protein would be predicted to cause a G1 cell cycle arrest of melanoma cells at concentrations indicative of their efficacy to down regulate MITF-M. To test this possibility, G361 melanoma cells were treated with 200 μ M I3C, 10 μ M 1-Benzyl-I3C or with the DMSO vehicle control for 48 hours and the potential cell cycle effects were analyzed by flow cytometry of propidium iodide-stained nuclear DNA. As shown in Figure 3B, indicative of a proliferative state, G361

cells treated with the DMSO vehicle control displayed cells in all phases of the cell cycle including approximately 50.1% cells in the G₁ phase. In contrast, treatment with 200 μ M I3C increased the percent of the percentage of cells with a G₁ DNA content in the overall cell population to 72.4%, which is consistent with a G₁ cell cycle arrest (Fig 3B, middle panel). Notably, treatment with 10 μ M 1-benzyl-I3C induced a G₁ cell arrest with 88.2 % of the total cells arrested in the G₁ phase of the cell cycle with relatively small numbers of cells remaining in the S and G₂/M cell cycle phases (Fig 3B, right panel). Taken together, our results show that 1-benzyl-I3C exhibits a significantly more effective anti-proliferative response compared to its parental compound I3C that generally reflects the increased efficacy for the inhibition of NEDD4-1 enzymatic activity. Therefore, we analyzed the interactions with NEDD4-1 and anti-proliferative response of additional synthetic indolecarbinol analogues with varying chemical properties.

3.4 Synthesis of I3C and 1-benzyl-I3C derivatives and in silico predicted interactions with the HECT domain of the NEDD4-1 ubiquitin ligase

To understand the molecular interactions between indolecarbinol compounds and the HECT domain of NEDD4-1, indolecarbinol analogues were designed to selectively alter chemical properties but maintain the benzene moiety that enables the 6 local C ^{δ^-} -H ^{δ^+} bond dipoles around the benzene ring to create an overall charge distribution that is composed of a negative charge in the center of the benzene ring that can bind cations. Also, each of the synthetic derivatives maintains the C-3 hydroxy methyl substituent that is important for the biological activity of the natural I3C parental compound [65]. In two analogs, methyl substituents were added at the para and ortho positions on the benzene ring forming (1-p-tolyl-1H-indol-3-yl)-carbinol (Fig.4, compound 2242)

and (1-o-tolyl-1H-indol-3-yl)-carbinol (Fig. 4, compound 2243), respectively. Each methyl group is electron donating, thus making the π system more nucleophilic and showing a higher propensity to participate in electrophilic substitution reactions. Two electron donating methoxy substituents were attached to the para and meta positions in the benzene ring forming (1-(3,4-dimethoxyphenyl)-1H-indol-3-yl) carbinol (Fig.4, compound 2244). The lone pairs of oxygen electrons on the dimethoxy groups are adjacent to the π system thereby increasing the electron density on the ring through a resonance donating effect that causes the π system to be more nucleophilic. In another indolecarbinol analogue, the linker carbon was eliminated from the benzyl group forming (1-phenyl-1H-indol-3-yl) carbinol (Fig.4, compound 2160), which makes the overall benzene moiety more rigid and less likely to participate in nucleophilic interactions. In the fifth derivative, a thiophene moiety was added to carbon 2 in the indole ring forming benzyl-2(thiophen-2-yl)-1H-indol-3-yl-carbinol (Fig.4, compound 2163). The thiophene group should add hydrophobic character but also significantly increases the bulkiness and decreases the flexibility of this analogue.

In silico computational modeling were performed to evaluate potential binding sites within NEDD4-1^{HECT} for each of the synthetic indolecarbinol analogues using the Schrödinger Induced Fit Docking protocol as described earlier. Simulations that dock each compound with NEDD4-1^{HECT} domain implicate several differences in selectivity between the synthetic indolecarbinol derivatives (Fig.5). For comparison, the predicted interactions of 1-benzyl-I3C is shown in Figure 5A. Each of indolecarbinol analogs is calculated to bind within the same binding cavity as I3C and 1-benzyl-I3C, which is adjacent to the N-lobe of the NEDD4-1 HECT domain. The π -system of the bound phenyl group in compound 2242 is predicted to engage in

an aromatic CH- π association with the aryl ring hydrogen of Phe 637. Potential hydrophobic associations are also observed between the compound's phenyl moiety and Met 600 (Fig.5B). Contrastingly, the methyl substituent placed in the ortho position on the phenyl ring of compound 2243 orients the compound such that it is predicted to make aryl-aryl interactions with Tyr 634 and van der Waals associations with Asn 628 and Glu 554 (Fig.5C). Compound 2244 is predicted to be anchored by hydrophobic residues Ile 596 and Leu 553 and is able to make aryl-aryl interactions with Tyr 557 and Tyr 634 via its 3,4, di-methoxy phenyl moiety. Compound 2244 is also predicted to associate with Arg 558 through cation- π bonds (Fig.5D). 2160 is predicted to engage in aryl-aryl interactions with Tyr 634 and Tyr 605 via the compound's indole moiety while its phenyl moiety is calculated to be anchored by hydrophobic residues Leu 607, Ile 638, and Ile 596 (Fig.5E). The thiophene moiety in compound 2163 is embedded between negatively charged residue Glu 554 and also engages in T-shaped edge-to-face interactions with Tyr 605. 2263 is also predicted to interact with hydrophobic residues Phe 637 and Met 600 via its phenyl moiety and is anchored between Tyr 634, Asn 628, and His 631 via its indole moiety (Fig. 5F).

All predicted interactions of the indolecarbinol analogs with specific amino acid residues of the NEDD4-1^{HECT} domain are within 4 Å of each compound. There are several amino acid residues of the HECT domain that are predicted to interact with all or most of the indolecarbinol analogs (Leu 553, Tyr 605, Leu 607, Cys 627, Asn 628, Tyr 634). The *in silico* analysis also uncovered predicted amino acid residue interactions that are relatively specific for selective sets of the indolecarbinol analogues (Tyr 557 and Phe 608 for Compounds 2242, 2243 and 2244; Ser 624 and His 631 for I3C, 1-benzyl-I3C and compound 2163; Glu 599 for compounds 2242, 2160

and 2163; Ile for compounds 2244 and 2160; Phe 601 for compounds 2243 and 2244; Phe 635 for I3C and compound 2242; Asn 602 for compounds 2243 and 2244; Asp 630 for 1-benzyl-I3C). Calculated docking scores for the *in silico* defined interactions of each indolecarbinol derivative with the NEDD4-1^{HECT} domain yielded negative values between approximately -11 kJ/mol and -6 kJ/mol, implicating that the ligand-protein structures are predicted to be generally stable. Simulations that used the C2 or WW domain structure of NEDD4-1 displayed no binding interactions with the indolecarbinol compounds (data not shown).

3.5 Binding of indolecarbinol analogs to the purified NEDD4-1^{HECT} domain of NEDD4-1.

The direct binding of each of the indolecarbinol analogs to the purified bacterially synthesized NEDD4-1^{HECT} domain was analyzed by Protein Thermal Shift assays described earlier for I3C and 1-benzyl-I3C. For comparative purposes, the Protein Thermal Shift melting profile for the NEDD4-1^{HECT} in the absence of added indolecarbinols (T_m of 47.9°C) and after addition of 1-benzyl-I3C (T_m of 58.1°C) from Figure 2C is incorporated into Figure 6. Exposure to all but one of the indolecarbinol compounds stabilized to different extents the NEDD4-1^{HECT} secondary structure based on concomitant increases in melting temperature Figure 6. From the protein melting temperatures profiles of NEDD4-1^{HECT} (Fig 6B), the compounds listed in descending melting temperatures or ΔT_m values are 1-benzyl-I3C (10.17°C), compound 2244 (9.47°C), compound 2242 (7.02°C), compound 2243 (5.26°C) and compound 2160 (1.76°C). Treatment of NEDD4-1^{HECT} with compound 2163 displayed a reduced (-2.00°C) peak melting temperature compared to the untreated NEDD4-1^{HECT}. These results show that each of the indolecarbinol compounds directly bind to the purified NEDD4-1^{HECT} domain, although the nature of the protein binding sites may differ, especially for the 2163 compound.

3.6 Inhibitory effects of the indolecarbinol analogs on the *in vitro* enzymatic activity of the NEDD4-1 ubiquitin ligase and anti-proliferative efficacy of human melanoma cells.

Each of the indolecarbinol analogues was preincubated with purified human NEDD4-1 protein for 1 hour and the *in vitro* polyubiquitylation assay described earlier was used to assess the effects on NEDD4-1 ubiquitin ligase activity. Compared to the effects of 1-benzyl-I3C from Figure 2E, the concentration-dependent effects of compounds 2242 and 2243 on NEDD4-1 enzymatic activity are shown in the upper left panel of Figure 7A, and the concentration-dependent effects of compounds 2244, 2160 and 2163 are shown in the upper right panel of Figure 7B. As a negative control, the level of NEDD4-1 enzymatic activity in the presence of 200 μ M tryptophol, a biologically inactive indolecarbinol [65], is also shown. Of the tested indolecarbinol analogues, compounds 2242 and 2243 were the most effective inhibitors of NEDD4-1 ubiquitin ligase activity. Compounds 2242 and 2243 each have electron donating methyl substituents added to different positions on benzene ring (see Fig 4). Their efficacies were similar to or slightly better than 1-benzyl-I3C and significantly greater than that of I3C (see Figure 2) with observed IC_{50} of 12.89 μ M for compound 2242 μ M, IC_{50} of 7.90 μ M for compound 2243 and IC_{50} of 12.34 μ M for 1-benzyl-I3C (summarized in Fig 9). The high potency of 2243, 2242, and 1-benzyl-I3C may be attributed to the addition of the phenyl moiety on the indole nitrogen of I3C that is predicted to form stabilizing cation- π interactions with basic residues within the HECT domain of NEDD4-1.

In contrast, compounds 2160, 2244 and 2163 have weaker inhibitory effects on NEDD4-1 catalytic activity compared to 1-benzyl-I3C with experimentally defined IC_{50} s of 30.4 μ M,

55.3 μM and 153 μM respectively. Based on the computational models, the substituents of the compounds 2163 and 2244 are solvent-exposed, and hence, unfavorable solvation of the bulky and hydrophobic groups may account for the reduced inhibitory activities compared to the 1-benzyl-I3C. Furthermore, the additional thiophene group attached to the indole ring in compound 2163 likely increases the compound's steric hindrance and prevents it from binding tightly to the protein, which likely accounts for the inhibitory effects on NEDD4-1 activity of 2163. These observations identify indolecarbinol analogs as a novel set of small molecule inhibitors of NEDD4-1 ubiquitin ligase activity.

Because of the connection between NEDD4-1 activity and the proliferation of G361 melanoma cells, the anti-proliferative effectiveness of 48 hour treatment with a concentration range of each of the indolecarbinol analogs was evaluated in comparison to 1-benzyl-I3C, I3C and the inactive indolecarbinol tryptophol. Melanoma cell proliferation was determined by CCK-8 proliferation assay that measures the number of cells. As shown in Figure 7C, the two most potent indolecarbinols were 1-benzyl-I3C and compound 2242 which displayed half maximal inhibition of melanoma cell proliferation of 14.7 μM and 18.3 μM , respectively (see Fig 9). The anti-proliferative efficacies of compounds 2243, 2244 and 2160 (half maximal responses of 25.1 μM , 40.0 μM and 47.1 μM , respectively) were intermediate between I3C and the two the highly potent molecules 1-benzyl-I3C and compound 2242. The anti-proliferative potency of compound 2163 displayed a generally similar half-maximal response as I3C (see Fig. 9). Tryptophol had no effect on melanoma cell proliferation, which is consistent with its lack of effects in other cancer cell types [32, 65]. Under the 48-hour treatment conditions used in these cell proliferation assays, there was no appreciable apoptosis observed, although treatment with

concentrations of each I3C analogue greater than those used for the dose responses seemed to trigger cellular apoptosis based on changes in cell morphology and loss of adhesion to the culture dish substratum (data not shown).

As another test of the anti-proliferative effects of the indolecarbinol analogues, melanoma cells were treated for 48 hours with increasing concentrations of the highly potent compound 2242 and the levels of phosphorylated and total Akt-1 protein were examined by western blots. As shown in Fig 7A (panel insert), compound 2242 strongly down regulated the level of phosphorylated Akt-1 compared to total Akt-1 protein levels. Densitometry of the western blot results was used to quantify the changes in phosphorylated Akt-1 to total Akt-1 protein at increasing concentrations of compound 2242. The results show that in a cellular context, the inhibition of NEDD4-1 enzymatic by this indolecarbinol analogue strongly correlated with the loss of phosphorylated and active Akt-1 (Fig 7A). We therefore propose that the down regulation of phosphorylated Akt-1 is associated with the mechanism driving the loss of cell proliferation by compound 2242 and presumably by the other tested synthetic indolecarbinol analogues.

Comparison of half maximal anti-proliferative responses in human melanoma cells and half maximal inhibition of NEDD4-1 enzymatic activities showed an overall correlation of the efficacies of both effects for the indolecarbinol analogues (Figure 9). One notable deviation of this correlation is with compound 2243 in which the relative inhibition of NEDD4-1 activity is more effective compared to its relative anti-proliferative response, which is likely caused by factors such as the efficiency of cellular import and stability of the indolecarbinol analogues. It

is also possible that the inhibition of NEDD4-1 activity triggers the anti-proliferative response. To assess whether the anti-proliferative responses of the new indolecarbinol analogues can be observed in human cancer cells derived from other tissue, human MCF-7 breast cancer cells were treated for 48 hours with a concentration range of each indolecarbinol analogue. MCF-7 cells were used for this analysis because we previously established that this cell line is highly sensitive to the anti-proliferative effects of I3C [31-33]. Breast cancer cell proliferation was determined by a CCK-8 proliferation assay as described earlier for the human melanoma cells. As shown in Figure 8, the most effective indolecarbinol compounds were 1-benzyl-I3C and compound 2244 which displayed a half maximal inhibition of breast cancer cell proliferation of 0.87 μ M and 32.10 μ M respectively. The anti-proliferative efficacies of compounds 2160, 2243, and 2242 (half maximal responses of 40.83 μ M, 58.44 μ M, 72.49 μ M, respectively) were intermediate between I3C and the two highly potent compounds 1-benzyl-I3C and compound 2244. The parental I3C compound had the least potent anti-proliferative effect with a half-maximal response of 157.32 μ M. Tryptophol had no effect on breast cancer cell proliferation.

4. Discussion

Regulation of cellular ubiquitination reactions through the activation or inhibition of individual ubiquitin ligases is an emerging potential strategy to target dysfunctional or hyperactive cellular processes in human cancer cells. One such intriguing therapeutic target is NEDD4-1, a HECT domain-containing ubiquitin ligase, which can display oncogenic-like properties through the targeted degradation of its protein substrates [1, 6]. However, relatively

little is known about small inhibitors of HECT domain-containing ubiquitin ligases, although conceivably the use of such inhibitors could potentially be used in the development of new anti-cancer strategies. Our results now demonstrate that the I3C and its synthetic derivatives are potent inhibitors of NEDD4-1 ubiquitin ligase activity and that the I3C indolecarbinol structure represents a novel chemical platform of small molecule inhibitors of HECT-domain-containing ubiquitin ligases. We examined the *in vitro* binding and inhibition of enzymatic activity of purified NEDD4-1 by I3C, 1-benzyl-I3C and of five additional synthetic indolecarbinol analogues that display selective alterations in the physical and chemical properties of the resulting indolecarbinol structure [31-33]. The enhanced ability of the indolecarbinol compounds to inhibit NEDD4-1 activity required an optimal nucleophilic π system within the benzene ring, whereas, functionality of the indolecarbinol analogues decreased with the loss of flexibility of the chemical scaffold. Also, each of the synthetic indolecarbinol compounds maintains the C-3 hydroxy methyl substituent that is important for the biological activity of the I3C parental compound [65]. The overall efficacy of the anti-proliferative effects in melanoma cells of the tested indolecarbinol compounds generally correlated with their *in vitro* inhibition of NEDD4-1 ubiquitin ligase activity, implicating the potential importance of the indolecarbinol structural scaffold in developing highly potent and stable anti-cancer molecules.

In silico computational simulations predict stable interactions of each of the indolecarbinol compounds with the catalytic HECT domain of NEDD4-1, whereas, the same analysis shows that the C2 and WW domains of NEDD4-1 do not contain any predicted indolecarbinol binding sites. NEDD4-1 enzymatic activity was strongly inhibited by treatment with 1-benzyl-I3C, compound 2242 and compound 2243, each of which have significant electron donating moieties attached to the

nitrogen position of the indole ring of I3C. Adding electron donating alkyl substituents to either the para or ortho positions on the benzene ring, forming compounds 2242 and 2243 respectively, produced the most potent inhibitors of NEDD4-1 enzymatic activity. This result suggests the importance of an optimal benzene ring nucleophilic π system for inhibiting enzymatic activity of NEDD4-1. In order to provide structural information for the indolecarbinol compounds in complex with NEDD4-1, we performed induced fit docking in the Schrödinger software suite to better understand the binding affinity of the protein-ligand complexes. While other docking programs have in the past been employed in structure-based drug design to optimize small molecule drug candidates, these programs assume that a flexible ligand is docked to a rigid receptor binding pocket, however, protein structural flexibility ought to be addressed due to the high dimensionality of the protein-ligand complex and to the dual nature of ligand binding sites which are defined by regions of high stability and high flexibility [66]. Indeed, the induced fit docking simulations predict highly stable interactions with the polar amino acid Asn 628 and hydrophobic amino acids Leu 607, Tyr 634, Tyr 605, Leu 553, Ile 638, Meth 600, and Phe 637 by compound 2242 and compound 2243 within the HECT domain of NEDD4-1. The addition of two electron donating methoxy substituents to the para and meta positions in the benzene ring forming compound 2244 resulted in an approximate 4.5-fold less potency compared to 1-benzyl-I3C but remained approximately 5-fold more potent than I3C. *In silico* modeling suggests that one reason for this reduced potency is the loss of predicted π stacking edge-to-face interactions with Tyr 634 and Tyr 605. Also, relative to 1-benzyl-I3C, compound 2244 is predicted to flip its orientation such that the indole ring is positioned where 1-benzyl-I3C's phenyl moiety was predicted to be located.

Compound 2160, in which the single carbon linker between the indolecarbinol nitrogen and the benzene ring was eliminated, reduced the 1-benzyl-I3C potency of NEDD4-1 activity inhibition by approximately 2.6-fold. The loss of the linker carbon causes the overall benzene moiety to be more rigid and less likely to participate in nucleophilic interactions, which further implicates the importance of maintaining the nucleophilic π system within the benzene ring for the inhibition of NEDD4-1 activity. The rigidity of compound 2160's benzene moiety causes it to adjust its position such that the benzene moiety is now predicted to lose its network of associations with critical residues Tyr 634, Asn 628, His 631 and Asp 630 that is predicted with 1-benzyl-I3C and instead forms weaker hydrophobic interactions with Ile 638 and Phe 637. The addition of the thiophene moiety to carbon 2 in the indole ring of 1-benzyl-I3C, forming compound 2163, generated an inhibitor of NEDD4-1 activity that is approximately equivalent to I3C and thereby reversed the enhanced efficacy of 1-benzyl-I3C. *In silico* modeling predicts that compound 2163's benzene moiety can maintain hydrophobic associations with residue Leu 607 but its thiophene moiety displaces interactions with Tyr 605 and Tyr 634 which is necessary for securely fastening compound 2163 at this pocket, and thus likely accounts for the loss of inhibitory activity of the 1-benzyl-I3C scaffold. Thus, although the thiophene moiety adds hydrophobic character, it also significantly increases the bulkiness and decreases the flexibility of the compound.

The predicted interactions of the indolecarbinol compounds with the NEDD4-1 HECT domain appears to be relatively specific for NEDD4-1 because the HECT domains in the HERC1, E6-AP, and ITCH families of ubiquitin ligases, which are only partially homologous to the NEDD4-1 HECT domain [67], show no *in silico* predicted interactions with I3C (data not shown). Consistent with the *in silico* docking analysis, protein thermal shift assays demonstrated

that each of indolecarbinol compounds bind *in vitro* to the purified NEDD4-1 HECT domain. The C2 and HECT domains of NEDD4-1, which are responsible for membrane localization and ubiquitin ligase activity respectively, bind each other resulting in an auto-inhibition of NEDD4-1 activity [68-70]. Conceivably, the indolecarbinol interactions with NEDD4-1 HECT domain could potentially inhibit NEDD4-1 activity by stabilizing the C2-HECT autoinhibitory intramolecular interactions or by preventing ubiquitin binding and poly ubiquitin chain elongation by forming tight aromatic associations with Tyr 605. An alternative hypothesis is that the indolecarbinol compounds may alter functional interactions of one or more NEDD4-1 upstream regulators that are thought to have context-specific effects on NEDD4-1 protein stabilization and activity depending on the transformed or stressed state of the cells [71, 72].

The indolecarbinol inhibition of NEDD4-1 enzymatic activity and disruption of downstream signaling probably accounts, in part, for the anti-proliferative effects of indolecarbinol molecules. Based on the known actions of I3C in human cancer cells [31-33], it is highly likely that synthetic indolecarbinol analogues of I3C regulate multiple cell signaling pathways in melanoma cells. In this regard, the most sensitive melanoma cells to the anti-proliferative effects of I3C express an oncogenic BRAF and a wild type form of PTEN [34, 39]. Oncogenic BRAF signaling maintains high levels of cellular Erk/MAPK activity whereas, PTEN down-regulates AKT signaling, which ultimately abolishes cell survival networks, anti-apoptotic and cell invasion properties of human melanoma cells [42, 73, 74]. The mechanistic relationship between NEDD4-1 ubiquitin ligase activity and PTEN protein has not been definitively established because of cell type-dependent differences in the resulting effects on PTEN protein ubiquitination, such as on protein stability and localization, as well as one report suggesting that

even though PTEN is a substrate of NEDD4-1, this ubiquitin ligase is regulated by PTEN signaling [75]. Several studies conclude that the oncogenic functions of NEDD4-1 are inversely linked to the tumor suppression functions of PTEN [5]. We have observed in wild type PTEN expressing melanoma cells, which also express an oncogenic BRAF, that the down regulation of NEDD4-1 activity either by I3C treatment or by siRNA knockdown of NEDD4-1 resulted in higher levels of wild type PTEN protein [34]. NEDD4-1 is frequently up regulated in a variety of human cancers [76], for example, in a majority of non-small cell lung cancer tumor tissues NEDD4-1 over expression correlated with the loss of PTEN protein [77]. In NHA-E6/E7/hTERT cells, expression of high levels of FoxM1B up regulated NEDD4-1, which led to the down regulation of PTEN and the hyperactivation of AKT [78].

The enhanced efficacy of the I3C analogues for their anti-proliferative properties is likely due to a combination of higher affinity and qualitatively more effective interactions with specific target proteins such as NEDD4-1 as well as potentially from enhanced cellular stability and more efficient uptake. In this regard, the addition of a benzene moiety to the position one nitrogen of the indole ring, forming 1-benzyl-I3C, prevents the self-condensation that occurs to different extents with the parental I3C compound [57]. Similarly, the highly potent compounds 2242 and 2243 are likely to be more stable in a cellular context and both are potentially highly promising anti-cancer molecules. Treatment with I3C activates distinct and overlapping sets of anti-proliferative signaling events in different cancer cell types [79], and the cell type selective responses of indolecarbinol compounds can be attributed to the presence and activity of individual indolecarbinol target proteins that regulate specific sets of cellular cascades. For example, we previously demonstrated that the I3C and 1-benzyl-I3C inhibition of elastase

enzymatic activity triggers anti-proliferative signaling in human breast cancer cells [33, 57] and I3C can inhibit oncogenic BRAF enzymatic activity and disrupt down stream signaling events in human melanoma cells [39]. The observed differences in the anti-proliferative effectiveness of each indolecarbinol compound in melanoma cells compared to breast cancer cells can conceivably be attributed to the different indolecarbinol target proteins expressed in each cell type with elastase being the most significant indolecarbinol target protein in human breast cancer cells [31-33], whereas NEDD4-1 and oncogenic BRAF being critical indolecarbinol target proteins in human melanoma cells [34, 39]. Conceivably, compound 2244, the most effective new indolecarbinol analogue in human breast cancer cells, may inhibit elastase more effectively and hence produce a stronger antiproliferative response in breast cancer cells compared to melanoma cells. We are currently attempting to dissect common structural features between the indolecarbinol target proteins that account for their sensitivities to I3C and its highly potent indolecarbinol analogues. Furthermore, because the vast majority of human melanoma cells express an oncogenic form of BRAF, the simultaneous disruption of NEDD4-1 and BRAF signaling by I3C and its derivatives implicates indolecarbinol analogs as intriguing new chemical foundations to develop highly potent, stable and target-specific anti-cancer compounds.

Conflict of Interest statement

The authors declare that there are no conflicts of interest.

Acknowledgments

This study is dedicated to the memory of Dr. Maria N. Preobrazhenskaya, a brilliant scientist and wonderful colleague who initiated our productive American-Russian collaboration.

The work was supported by National Institutes of Health Public Service grant CA164095 awarded from the National Cancer Institute and by a grant from the Russian Scientific Foundation (project No. 16-15-10300). We would like to thank members of both the Firestone and the Preobrazhenskaya laboratories for their outstanding advice and timely suggestions during the course of this work.

References

- [1] Ravid T, Hochstrasser M: Diversity of degradation signals in the ubiquitin-proteasome system. *Nat Rev Mol Cell Biol* 2008, 9(9):679-690.
- [2] Rotin D, Kumar S: Physiological functions of the HECT family of ubiquitin ligases. *Nat Rev Mol Cell Biol* 2009, 10(6):398-409.
- [3] Bernassola F, Karin M, Ciechanover A, Melino G: The HECT family of E3 ubiquitin ligases: multiple players in cancer development. *Cancer Cell* 2008, 14(1):10-21.
- [4] Yang B, Kumar S: Nedd4 and Nedd4-2: closely related ubiquitin-protein ligases with distinct physiological functions. *Cell Death Differ* 2010, 17(1):68-77.
- [5] Ye X, Wang L, Shang B, Wang Z, Wei W: NEDD4: a promising target for cancer therapy. *Curr Cancer Drug Targets* 2014, 14(6):549-556.
- [6] Katz M, Shtiegman K, Tal-Or P, Yakir L, Mosesson Y, Harari D, Machluf Y, Asao H, Jovin T, Sugamura K *et al*: Ligand-independent degradation of epidermal growth factor receptor involves receptor ubiquitylation and Hgs, an adaptor whose ubiquitin-interacting motif targets ubiquitylation by Nedd4. *Traffic* 2002, 3(10):740-751.

- [7] Aggarwal BB, Ichikawa H: Molecular targets and anticancer potential of indole-3-carbinol and its derivatives. *Cell Cycle* 2005, 4(9):1201-1215.
- [8] Ahmad A, Sakr WA, Rahman KMW: Anticancer Properties of Indole Compounds: Mechanism of Apoptosis Induction and Role in Chemotherapy. *Curr Drug Targets* 2010, 11(6):652-666.
- [9] Moiseeva EP, Almeida GM, Jones GD, Manson MM: Extended treatment with physiologic concentrations of dietary phytochemicals results in altered gene expression, reduced growth, and apoptosis of cancer cells. *Mol Cancer Ther* 2007, 6(11):3071-3079.
- [10] Hsu JC, Dev A, Wing A, Brew CT, Bjeldanes LF, Firestone GL: Indole-3-carbinol mediated cell cycle arrest of LNCaP human prostate cancer cells requires the induced production of activated p53 tumor suppressor protein. *Biochem Pharmacol* 2006, 72(12):1714-1723.
- [11] Melkamu T, Zhang XX, Tan JK, Zeng Y, Kassie F: Alteration of microRNA expression in vinyl carbamate-induced mouse lung tumors and modulation by the chemopreventive agent indole-3-carbinol. *Carcinogenesis* 2010, 31(2):252-258.
- [12] Kim DS, Jeong YM, Moon SI, Kim SY, Kwon SB, Park ES, Youn SW, Park KC: Indole-3-carbinol enhances ultraviolet B-induced apoptosis by sensitizing human melanoma cells. *Cell Mol Life Sci* 2006, 63(22):2661-2668.
- [13] Machijima Y, Ishikawa C, Sawada S, Okudaira T, Uchihara JN, Tanaka Y, Taira N, Mori N: Anti-adult T-cell leukemia/lymphoma effects of indole-3-carbinol. *Retrovirology* 2009, 6.
- [14] Qi M, Anderson AE, Chen DZ, Sun S, Auborn KJ: Indole-3-carbinol prevents PTEN loss in cervical cancer in vivo. *Mol Med* 2005, 11(1-12):59-63.

- [15] Jin L, Qi M, Chen DZ, Anderson A, Yang GY, Arbeit JM, Auborn KJ: Indole-3-carbinol prevents cervical cancer in human papilloma virus type 16 (HPV16) transgenic mice. *Cancer Res* 1999, 59(16):3991-3997.
- [16] Cover CM, Hsieh SJ, Tran SH, Hallden G, Kim GS, Bjeldanes LF, Firestone GL: Indole-3-carbinol inhibits the expression of cyclin-dependent kinase-6 and induces a G1 cell cycle arrest of human breast cancer cells independent of estrogen receptor signaling. *J Biol Chem* 1998, 273(7):3838-3847.
- [17] Sarkar FH, Li Y: Indole-3-carbinol and prostate cancer. *J Nutr* 2004, 134(12 Suppl):3493S-3498S.
- [18] Firestone GL, Bjeldanes LF: Indole-3-carbinol and 3-3'-diindolylmethane antiproliferative signaling pathways control cell-cycle gene transcription in human breast cancer cells by regulating promoter-Sp1 transcription factor interactions. *J Nutr* 2003, 133(7 Suppl):2448S-2455S.
- [19] Firestone GL, Sundar SN: Minireview: Modulation of Hormone Receptor Signaling by Dietary Anticancer Indoles. *Mol Endocrinol* 2009, 23(12):1940-1947.
- [20] Marconett CN, Sundar SN, Poindexter KM, Stueve TR, Bjeldanes LF, Firestone GL: Indole-3-carbinol triggers aryl hydrocarbon receptor-dependent estrogen receptor (ER)alpha protein degradation in breast cancer cells disrupting an ERalpha-GATA3 transcriptional cross-regulatory loop. *Mol Biol Cell* 2010, 21(7):1166-1177.
- [21] Marconett CN, Sundar SN, Tseng M, Tin AS, Tran KQ, Mahuron KM, Bjeldanes LF, Firestone GL: Indole-3-carbinol downregulation of telomerase gene expression requires the inhibition of estrogen receptor-alpha and Sp1 transcription factor interactions within

- the hTERT promoter and mediates the G(1) cell cycle arrest of human breast cancer cells. *Carcinogenesis* 2011, 32(9):1315-1323.
- [22] Maruthanila VL, Poornima J, Mirunalini S: Attenuation of Carcinogenesis and the Mechanism Underlying by the Influence of Indole-3-carbinol and Its Metabolite 3,3'-Diindolylmethane: A Therapeutic Marvel. *Adv Pharmacol Sci* 2014, 2014:832161.
- [23] Sarkar FH, Li Y, Wang Z, Kong D: Cellular signaling perturbation by natural products. *Cell Signal* 2009, 21(11):1541-1547.
- [24] Xu Y, Zhang J, Dong WG: Indole-3-carbinol (I3C)-induced apoptosis in nasopharyngeal cancer cells through Fas/FasL and MAPK pathway. *Med Oncol* 2011, 28(4):1343-1348.
- [25] Aggarwal BB, Shishodia S: Molecular targets of dietary agents for prevention and therapy of cancer. *Biochemical Pharmacology* 2006, 71(10):1397-1421.
- [26] Kim YS, Milner JA: Targets for indole-3-carbinol in cancer prevention. *J Nutr Biochem* 2005, 16(2):65-73.
- [27] Rogan EG: The natural chemopreventive compound indole-3-carbinol: State of the science. *In Vivo* 2006, 20(2):221-228.
- [28] Auborn KJ, Fan S, Rosen EM, Goodwin L, Chandrasekaran A, Williams DE, Chen D, Carter TH: Indole-3-carbinol is a negative regulator of estrogen. *J Nutr* 2003, 133(7 Suppl):2470S-2475S.
- [29] Wang TT, Milner MJ, Milner JA, Kim YS: Estrogen receptor alpha as a target for indole-3-carbinol. *J Nutr Biochem* 2006, 17(10):659-664.
- [30] Weng JR, Tsai CH, Kulp SK, Chen CS: Indole-3-carbinol as a chemopreventive and anti-cancer agent. *Cancer Lett* 2008, 262(2):153-163.

- [31] Nguyen HH, Aronchik I, Brar GA, Nguyen DH, Bjeldanes LF, Firestone GL: The dietary phytochemical indole-3-carbinol is a natural elastase enzymatic inhibitor that disrupts cyclin E protein processing. *Proc Natl Acad Sci U S A* 2008, 105(50):19750-19755.
- [32] Aronchik I, Bjeldanes LF, Firestone GL: Direct inhibition of elastase activity by indole-3-carbinol triggers a CD40-TRAF regulatory cascade that disrupts NF-kappaB transcriptional activity in human breast cancer cells. *Cancer Res* 2010, 70(12):4961-4971.
- [33] Aronchik I, Chen T, Durkin KA, Horwitz MS, Preobrazhenskaya MN, Bjeldanes LF, Firestone GL: Target protein interactions of indole-3-carbinol and the highly potent derivative 1-benzyl-I3C with the C-terminal domain of human elastase uncouples cell cycle arrest from apoptotic signaling. *Mol Carcinog* 2012, 51(11):881-894.
- [34] Aronchik I, Kundu A, Quirit JG, Firestone GL: The antiproliferative response of indole-3-carbinol in human melanoma cells is triggered by an interaction with NEDD4-1 and disruption of wild-type PTEN degradation. *Mol Cancer Res* 2014, 12(11):1621-1634.
- [35] Nemoto E, Tada H, Shimauchi H: Disruption of CD40/CD40 ligand interaction with cleavage of CD40 on human gingival fibroblasts by human leukocyte elastase resulting in down-regulation of chemokine production. *J Leukoc Biol* 2002, 72(3):538-545.
- [36] Tong AW, Papayoti MH, Netto G, Armstrong DT, Ordonez G, Lawson JM, Stone MJ: Growth-inhibitory effects of CD40 ligand (CD154) and its endogenous expression in human breast cancer. *Clin Cancer Res* 2001, 7(3):691-703.
- [37] Zhou Y, Eppenberger-Castori S, Eppenberger U, Benz CC: The NFkappaB pathway and endocrine-resistant breast cancer. *Endocr Relat Cancer* 2005, 12 Suppl 1:S37-46.

- [38] Madhusoodhanan R, Natarajan M, Veeraraghavan J, Herman TS, Aravindan N: NF κ B activity and transcriptional responses in human breast adenocarcinoma cells after single and fractionated irradiation. *Cancer Biol Ther* 2009, 8(9):765-773.
- [39] Kundu A, Quirit JG, Khouri MG, Firestone GL: Inhibition of oncogenic BRAF activity by indole-3-carbinol disrupts microphthalmia-associated transcription factor expression and arrests melanoma cell proliferation. *Mol Carcinog* 2016.
- [40] Aguisa-Toure AH, Li G: Genetic alterations of PTEN in human melanoma. *Cell Mol Life Sci* 2012, 69(9):1475-1491.
- [41] Conde-Perez A, Larue L: PTEN and melanomagenesis. *Future Oncol* 2012, 8(9):1109-1120.
- [42] Hodis E, Watson IR, Kryukov GV, Arolt ST, Imielinski M, Theurillat JP, Nickerson E, Auclair D, Li L, Place C *et al*: A landscape of driver mutations in melanoma. *Cell* 2012, 150(2):251-263.
- [43] Zhang H, Cai Q, Ma D: Amino acid promoted CuI-catalyzed C-N bond formation between aryl halides and amines or N-containing heterocycles. *J Org Chem* 2005, 70(13):5164-5173.
- [44] Holla BS, Ambekar SY: Studies in Biheterocycles .1. Formylation of 2-(2'-Thienyl) Indole. *J Indian Chem Soc* 1974, 51(11):965-966.
- [45] Niesen FH, Berglund H, Vedadi M: The use of differential scanning fluorimetry to detect ligand interactions that promote protein stability. *Nat Protoc* 2007, 2(9):2212-2221.
- [46] Kathman SG, Span I, Smith AT, Xu Z, Zhan J, Rosenzweig AC, Statsyuk AV: A Small Molecule That Switches a Ubiquitin Ligase From a Processive to a Distributive Enzymatic Mechanism. *J Am Chem Soc* 2015, 137(39):12442-12445.

- [47] Sastry GM, Adzhigirey M, Day T, Annabhimoju R, Sherman W: Protein and ligand preparation: parameters, protocols, and influence on virtual screening enrichments. *J Comput Aided Mol Des* 2013, 27(3):221-234.
- [48] Farid R, Day T, Friesner RA, Pearlstein RA: New insights about HERG blockade obtained from protein modeling, potential energy mapping, and docking studies. *Bioorg Med Chem* 2006, 14(9):3160-3173.
- [49] Sherman W, Day T, Jacobson MP, Friesner RA, Farid R: Novel procedure for modeling ligand/receptor induced fit effects. *J Med Chem* 2006, 49(2):534-553.
- [50] Sherman W, Beard HS, Farid R: Use of an induced fit receptor structure in virtual screening. *Chem Biol Drug Des* 2006, 67(1):83-84.
- [51] Jacobson MP, Pincus DL, Rapp CS, Day TJ, Honig B, Shaw DE, Friesner RA: A hierarchical approach to all-atom protein loop prediction. *Proteins* 2004, 55(2):351-367.
- [52] Jacobson MP, Friesner RA, Xiang ZX, Honig B: On the role of the crystal environment in determining protein side-chain conformations. *J Mol Biol* 2002, 320(3):597-608.
- [53] Hershko A, Ciechanover A: The ubiquitin system. *Annu Rev Biochem* 1998, 67:425-479.
- [54] Welchman RL, Gordon C, Mayer RJ: Ubiquitin and ubiquitin-like proteins as multifunctional signals. *Nat Rev Mol Cell Biol* 2005, 6(8):599-609.
- [55] Ciechanover A: The ubiquitin-proteasome pathway: on protein death and cell life. *EMBO J* 1998, 17(24):7151-7160.
- [56] Raasi S, Varadan R, Fushman D, Pickart CM: Diverse polyubiquitin interaction properties of ubiquitin-associated domains. *Nat Struct Mol Biol* 2005, 12(8):708-714.
- [57] Nguyen HH, Lavrenov SN, Sundar SN, Nguyen DH, Tseng M, Marconett CN, Kung J, Staub RE, Preobrazhenskaya MN, Bjeldanes LF *et al*: 1-Benzyl-indole-3-carbinol is a

- novel indole-3-carbinol derivative with significantly enhanced potency of anti-proliferative and anti-estrogenic properties in human breast cancer cells. *Chem Biol Interact* 2010, 186(3):255-266.
- [58] Maspero E, Mari S, Valentini E, Musacchio A, Fish A, Pasqualato S, Polo S: Structure of the HECT:ubiquitin complex and its role in ubiquitin chain elongation. *EMBO Rep* 2011, 12(4):342-349.
- [59] Vedadi M, Niesen FH, Allali-Hassani A, Fedorov OY, Finerty PJ, Jr., Wasney GA, Yeung R, Arrowsmith C, Ball LJ, Berglund H *et al*: Chemical screening methods to identify ligands that promote protein stability, protein crystallization, and structure determination. *Proc Natl Acad Sci U S A* 2006, 103(43):15835-15840.
- [60] Regad T: Molecular and cellular pathogenesis of melanoma initiation and progression. *Cell Mol Life Sci* 2013, 70(21):4055-4065.
- [61] Levy C, Khaled M, Fisher DE: MITF: master regulator of melanocyte development and melanoma oncogene. *Trends Mol Med* 2006, 12(9):406-414.
- [62] Pierrat MJ, Marsaud V, Mauviel A, Javelaud D: Expression of microphthalmia-associated transcription factor (MITF), which is critical for melanoma progression, is inhibited by both transcription factor GLI2 and transforming growth factor-beta. *J Biol Chem* 2012, 287(22):17996-18004.
- [63] Du J, Widlund HR, Horstmann MA, Ramaswamy S, Ross K, Huber WE, Nishimura EK, Golub TR, Fisher DE: Critical role of CDK2 for melanoma growth linked to its melanocyte-specific transcriptional regulation by MITF. *Cancer Cell* 2004, 6(6):565-576.

- [64] Wellbrock C, Rana S, Paterson H, Pickersgill H, Brummelkamp T, Marais R: Oncogenic BRAF regulates melanoma proliferation through the lineage specific factor MITF. *PLoS One* 2008, 3(7):e2734.
- [65] Jump SM, Kung J, Staub R, Kinseth MA, Cram EJ, Yudina LN, Preobrazhenskaya MN, Bjeldanes LF, Firestone GL: N-Alkoxy derivatization of indole-3-carbinol increases the efficacy of the G1 cell cycle arrest and of I3C-specific regulation of cell cycle gene transcription and activity in human breast cancer cells. *Biochem Pharmacol* 2008, 75(3):713-724.
- [66] Luque I, Freire E: Structural stability of binding sites: Consequences for binding affinity and allosteric effects. *Proteins-Structure Function and Genetics* 2000:63-71.
- [67] Scheffner M, Kumar S: Mammalian HECT ubiquitin-protein ligases: biological and pathophysiological aspects. *Biochim Biophys Acta* 2014, 1843(1):61-74.
- [68] Wang J, Peng Q, Lin Q, Childress C, Carey D, Yang W: Calcium activates Nedd4 E3 ubiquitin ligases by releasing the C2 domain-mediated auto-inhibition. *J Biol Chem* 2010, 285(16):12279-12288.
- [69] Wiesner S, Ogunjimi AA, Wang HR, Rotin D, Sicheri F, Wrana JL, Forman-Kay JD: Autoinhibition of the HECT-type ubiquitin ligase Smurf2 through its C2 domain. *Cell* 2007, 130(4):651-662.
- [70] Snyder PM, Olson DR, McDonald FJ, Bucher DB: Multiple WW domains, but not the C2 domain, are required for inhibition of the epithelial Na⁺ channel by human Nedd4. *J Biol Chem* 2001, 276(30):28321-28326.

- [71] Oberst A, Malatesta M, Aqeilan RI, Rossi M, Salomoni P, Murillas R, Sharma P, Kuehn MR, Oren M, Croce CM *et al*: The Nedd4-binding partner 1 (N4BP1) protein is an inhibitor of the E3 ligase Itch. *Proc Natl Acad Sci U S A* 2007, 104(27):11280-11285.
- [72] Schieber C, Howitt J, Putz U, White JM, Parish CL, Donnelly PS, Tan SS: Cellular up-regulation of Nedd4 family interacting protein 1 (Ndfip1) using low levels of bioactive cobalt complexes. *J Biol Chem* 2011, 286(10):8555-8564.
- [73] Chakraborty R, Wieland CN, Comfere NI: Molecular targeted therapies in metastatic melanoma. *Pharmgenomics Pers Med* 2013, 6:49-56.
- [74] Bandarchi B, Jabbari CA, Vedadi A, Navab R: Molecular biology of normal melanocytes and melanoma cells. *J Clin Pathol* 2013, 66(8):644-648.
- [75] Ahn Y, Hwang CY, Lee SR, Kwon KS, Lee C: The tumour suppressor PTEN mediates a negative regulation of the E3 ubiquitin-protein ligase Nedd4. *Biochem J* 2008, 412(2):331-338.
- [76] Chen C, Matesic LE: The Nedd4-like family of E3 ubiquitin ligases and cancer. *Cancer Metastasis Rev* 2007, 26(3-4):587-604.
- [77] Amodio N, Scrima M, Palaia L, Salman AN, Quintiero A, Franco R, Botti G, Pirozzi P, Rocco G, De Rosa N *et al*: Oncogenic role of the E3 ubiquitin ligase NEDD4-1, a PTEN negative regulator, in non-small-cell lung carcinomas. *Am J Pathol* 2010, 177(5):2622-2634.
- [78] Dai B, Pieper RO, Li D, Wei P, Liu M, Woo SY, Aldape KD, Sawaya R, Xie K, Huang S: FoxM1B regulates NEDD4-1 expression, leading to cellular transformation and full malignant phenotype in immortalized human astrocytes. *Cancer Res* 2010, 70(7):2951-2961.

- [79] Gupta SC, Kim JH, Prasad S, Aggarwal BB: Regulation of survival, proliferation, invasion, angiogenesis, and metastasis of tumor cells through modulation of inflammatory pathways by nutraceuticals. *Cancer Metastasis Rev* 2010, 29(3):405-434.

Figure Legends

Fig. 1. Synthesis and characterization of I3C analogues LCTA-2160, LCTA-2242, LCTA-2243, LCTA-2244 and LCTA-2163. The substituents attached on the benzene ring are represented as R= H (a); p-CH₃ (b); o-CH₃ (c); m,p-di OCH₃ (d). The reagents used for each step in the scheme are as follows: i) CuI; L-Proline; K₂CO₃; DMSO; ii) POCl₃; DMF; iii) NaBH₄; ethanol; iv) DMSO, KOH **A**) Scheme 1. Synthesis of compounds **5 a-d** where (**5a**) denotes LCTA-2160 ; (**5b**) denotes LCTA-2242 ; (**5c**) denotes LCTA-2243 ; (**5d**) denotes LCTA-2244 **B**) Scheme 2. Synthesis of LCTA-2163, denoted as (**5e**)

Fig. 2. *In silico* computational modeling of predicted molecular interactions of I3C and 1-benzyl-I3C with human NEDD4-1 HECT domain. (A & B) The 3D crystal structure of NEDD4-1 HECT domain (PDB accession number: 5C91) and the corresponding indolecarbinol compounds (shown in 1A: I3C; 1B: 1-benzyl-I3C) were processed with the Protein Preparation Wizard in the Schrödinger suite and were evaluated using the Schrödinger induced fit docking (IFD) protocol to represent conformational changes in the ligand binding site stimulated by ligand binding. Close contact residues are labeled and are within 4 Å of each indolecarbinol compound. Models were visualized using PyMol. (C) Binding of I3C or 1-benzyl-I3C to purified NEDD4-1 HECT domain was evaluated via protein thermal shift assays. The first derivative melt profiles show melting temperatures of NEDD4-1 HECT domain in the absence or presence of either 25 µM 1-benzyl-I3C or 250 µM I3C. Data is expressed as average of triplicate experiments. (D) Quantification of purified NEDD4-1 E3 ligase activity was determined via an ELISA based polyubiquitination assay as described in the Methods. Assay functionality was validated by

assessing polyubiquitination activity in the absence or presence of NEDD4-1. (E) Purified NEDD4-1 was pre-incubated with the indicated concentrations of I3C, 1-benzyl-I3C, or tryptophol for 1 hr and subsequently transferred to an ELISA microplate where the remaining contents of the reaction (E1, E2, and ubiquitin) were added. The *in vitro* formation of poly-ubiquitin chains was analyzed in an ELISA microplate and the enzymatic reactions were initiated with ATP. The washed plates were first incubated with biotin-linked ubiquitin antibody and then incubated with streptavidin-HRP to monitor NEDD4-1 auto-ubiquitination as the readout for NEDD4-1 activity. Enhanced chemiluminescent (ECL) reagent was then added to each well and incubated for 5 min. The relative light units (RLUs) were recorded using an LMax II/II384 microplate luminometer. NEDD4-1 enzymatic activity was standardized to the untreated NEDD4-1 protein and the data are expressed as the average of triplicate \pm SD.

Fig. 3. Effects of I3C and 1-benzyl-I3C on MITF-M protein levels and cell cycle in G361 human melanoma cells. (A) Western blot analysis of the effects of I3C and 1-benzyl-I3C on protein expression of MITF and in G361 cells. G361 cells were treated for 48 hours with the indicated concentrations of I3C or 1-benzyl-I3C. Cells were lysed, electrophoretically fractionated and western blots probed for MITF-M protein. HSP-90 was used as a loading control (left panel). The relative levels of MITF-M protein under each condition were quantified by densitometry of the western blots and normalized to the HSP-90 loading control protein (right panel). (B) G361 melanoma cells treated for 48 hr with the DMSO vehicle control, 200 μ M I3C, or 10 μ M 1-benzyl-I3C and the cell population DNA contents were quantified by flow cytometry of propidium stained nuclei. Representative flow histogram of each set of cells is shown in the panel. The data represents as an average of 3 independent experiments, performed in triplicate.

Fig. 4. Structures of I3C, 1-benzyl-I3C, and indolecarbinol analogues. Each of the synthetic analogs maintains the C-3 hydroxy methyl substituent. Methyl substituents were added at the para and ortho positions on the benzene ring forming (1-*p*-tolyl-1H-indol-3-yl)-carbinol (compound 2242) and (1-*o*-tolyl-1H-indol-3-yl)-carbinol (compound 2243), respectively. Two methoxy substituents were attached to the para and meta positions in the benzene ring forming (1-(3,4-dimethoxyphenyl)-1H-indol-3-yl) carbinol (compound 2244). The linker carbon was eliminated from the benzyl group forming (1-phenyl-1H-indol-3-yl) carbinol (compound 2160). A thiophene moiety was added to carbon 2 in the indole ring forming benzyl-2(thiophen-2-yl)-1H-indol-3-yl-carbinol (compound 2163).

Fig. 5 *In silico* computational models of predicted molecular interactions of (A) 1-benzyl-I3C, (B) 2242, (C) 2243, (D) 2244, (E) 2160, and (F) 2163 with the human NEDD4-1 HECT domain x-ray crystal structure (PDB accession number: 5C91). The structures of NEDD4-1 HECT domain and the corresponding indolecarbinol compounds (shown in 1A: I3C; 1B: 1-benzyl-I3C) were processed with the Protein Preparation Wizard in the Schrödinger suite and were evaluated using the Schrödinger induced fit docking (IFD) protocol to represent conformational changes in the ligand binding site stimulated by ligand binding. Close contact residues are labeled and are within 4 Å of each indolecarbinol compound. Models were visualized using PyMol.

Fig. 6 Binding of indolecarbinol compounds to purified NEDD4-1 HECT domain was evaluated via protein thermal shift assays. (A) The first derivative melt profiles show melting temperatures of NEDD4-1 HECT domain in the absence or presence of either 25 µM 1-benzyl-I3C, 2242, or 2243,

or 250 μ M I3C, 2244, 2160, or 2163. An increase in melting temperature is indicative of enhanced protein thermostability due to indolecarbinol binding. (B) Bar graph depicts changes in melting temperature of NEDD4-1 HECT domain in the presence of each respective indolecarbinol compound. Data is expressed as average of triplicate experiments and significance was assigned at a * p value < 0.05; ** p < 0.01; *** p <0.001 where each group was compared to control protein with no additions; NS, no significant difference compared to control.

Fig. 7 Effects of indolecarbinol compounds on the *in vitro* enzymatic activity of NEDD4-1 and on G361 human melanoma cell proliferation. (A & B) Purified NEDD4-1 was pre-incubated with the indicated concentrations of each indolecarbionol compound for 1 hr and each mixture subsequently transferred to an ELISA microplate where the remaining contents of the ubiquitination reaction (E1, E2, and ubiquitin) were added. The formation of poly-ubiquitin chains was analyzed in an ELISA microplate and the enzymatic reactions were initiated with ATP. The washed plates were first incubated with biotin-linked ubiquitin antibody and then incubated with streptavidin-HRP to monitor NEDD4-1 auto-ubiquitination as the readout for NEDD4-1 activity. Enhanced chemiluminescent (ECL) reagent was then added to each well and incubated for 5 min. The relative light units (RLUs) were recorded using an LMax II/II384 microplate luminometer. NEDD4-1 enzymatic activity was standardized to the untreated NEDD4-1 protein and the data are expressed as the average of triplicate \pm SD. Comparison of Tryptophol, 1-benzyl-I3C, 2242, and 2243 is shown in panel A and comparison of Tryptophol, 1-benzyl-I3C, 2244, 2160, and 2163 is shown in panel B. The insert to Figure 7A shows the protein levels of phosphorylated Akt-1 (pAKT-1), total Akt-1, and the HSP-90 gel-loading control that were determined by Western blot analysis of electrophoretically fractionated total

cell extracts after G-361 melanoma cells were treated with the indicated concentrations of compound 2242 for 48 hours. The relative levels of phosphorylated Akt-1 protein compared to the levels of total Akt-1 protein was quantified by densitometry of the western blots and the results shown as relative densitometry units compared to untreated cells. (C & D) The concentration dependent effects of 48 hr treatment of indolecarbinol compounds on the proliferation of G361 melanoma cells. Absorbance at 450 nm monitored the relative cell number and the values were determined by standardizing the average of each treatment triplicate to the average value observed in vehicle control treated melanoma cells. The data show the average of 3 independent experiments. Comparison of Tryptophol, I3C, 1-benzyl-I3C, 2242, and 2243 is shown in panel C and the comparison of Tryptophol, I3C, 1-benzyl-I3C, 2244, 2160, and 2163 is shown in panel D.

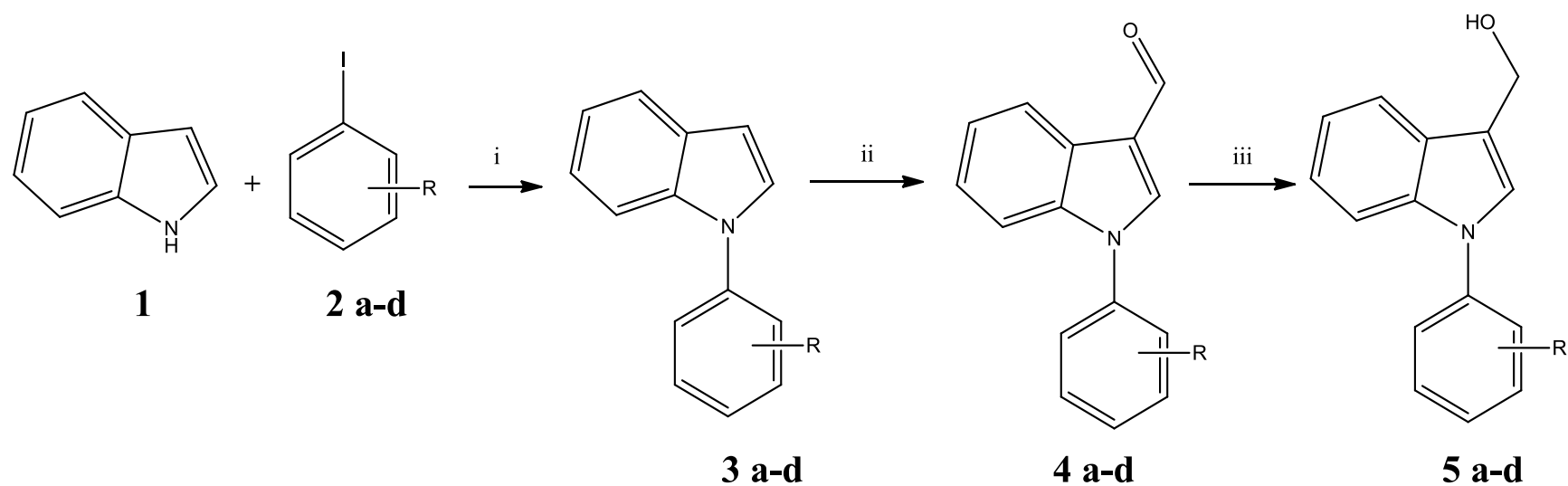
Fig. 8. The concentration dependent effect of the indolecarbinal analogues on the proliferation of MCF-7 breast cancer cells. Cells were treated for 48 hours with the indicated concentrations of I3C, 1-benzyl-I3C and the other synthetic I3C analogues. Absorbance at 450 nm monitored the relative cell number and the values were determined by standardizing the average of each treatment triplicate to the average value observed in vehicle control treated melanoma cells. The data show the average of 3 independent experiments.

Fig. 9. Table comparing the half maximum inhibitory concentration for NEDD4-1 enzymatic activity after 1 hr treatment and half maximum inhibition of proliferation of G361 cells after 48 hours treatment with each indolecarbinol compound. The data was processed using GraphPad Prism 6 non-linear regression analysis.

Figure 1

A

Scheme 1



B

Scheme 2

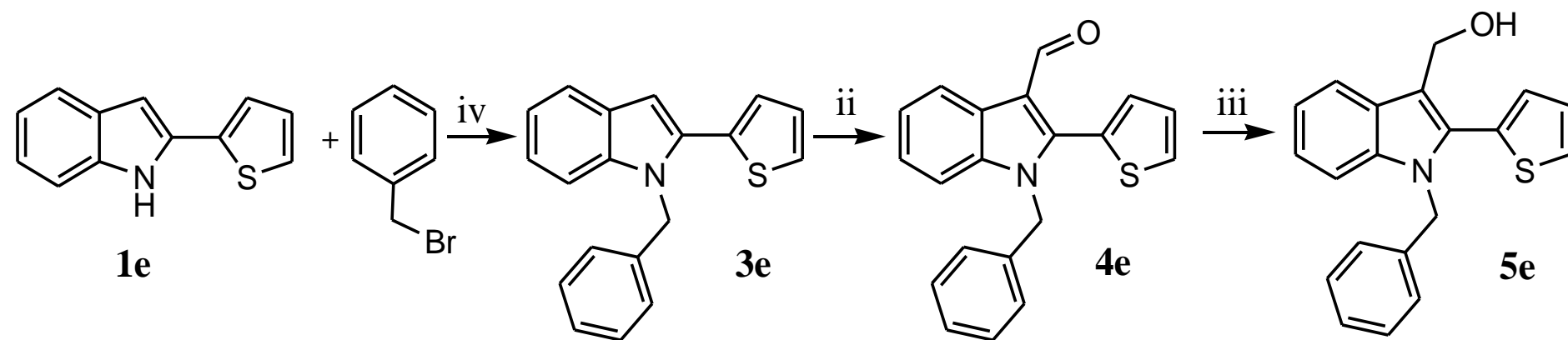
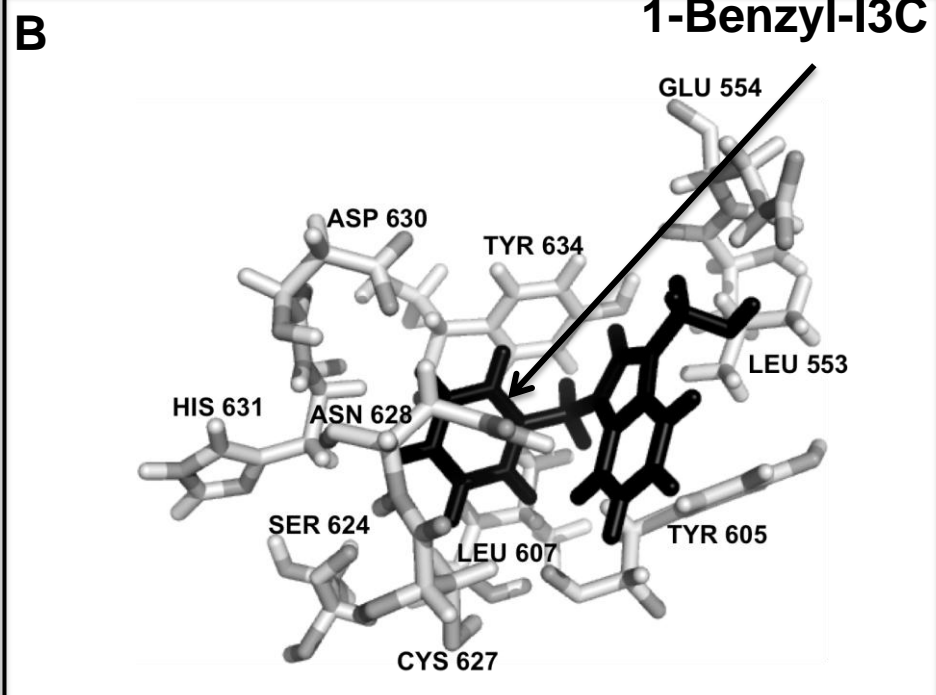
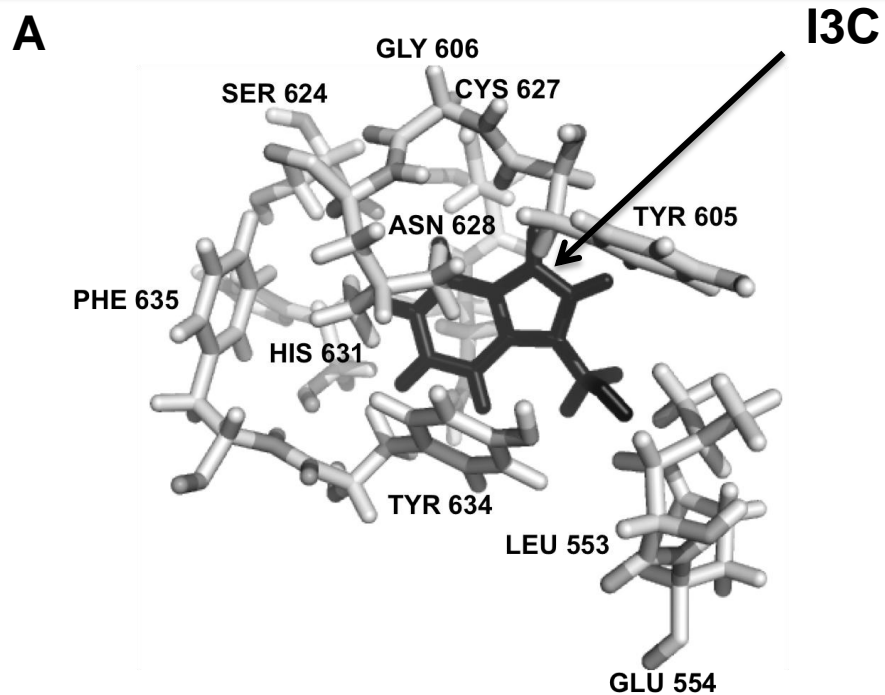
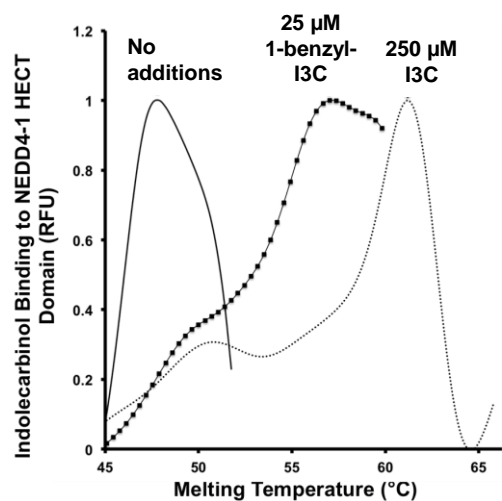


Figure 2



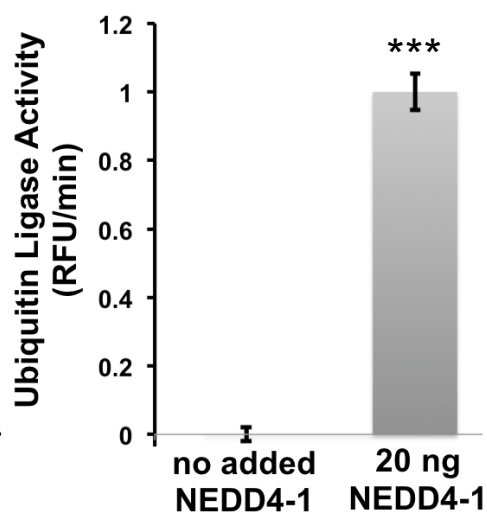
C

Protein Thermal Shift Assay



D

Ubiquitin Ligase Activity



E

I3C
 IC_{50} : 284 μ M

1-benzyl-I3C
 IC_{50} : 12.3 μ M

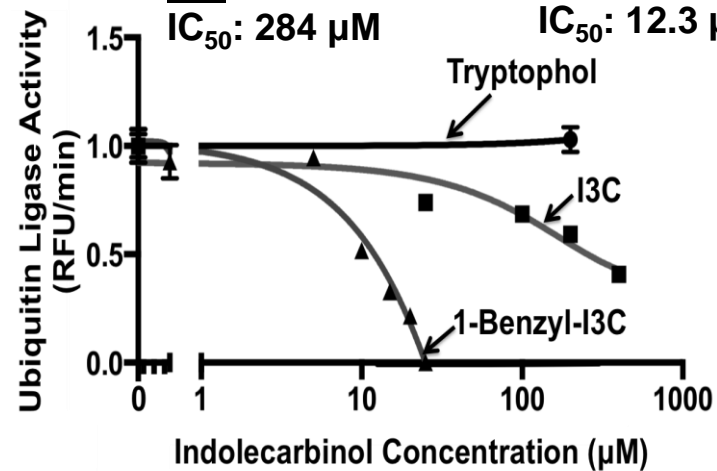
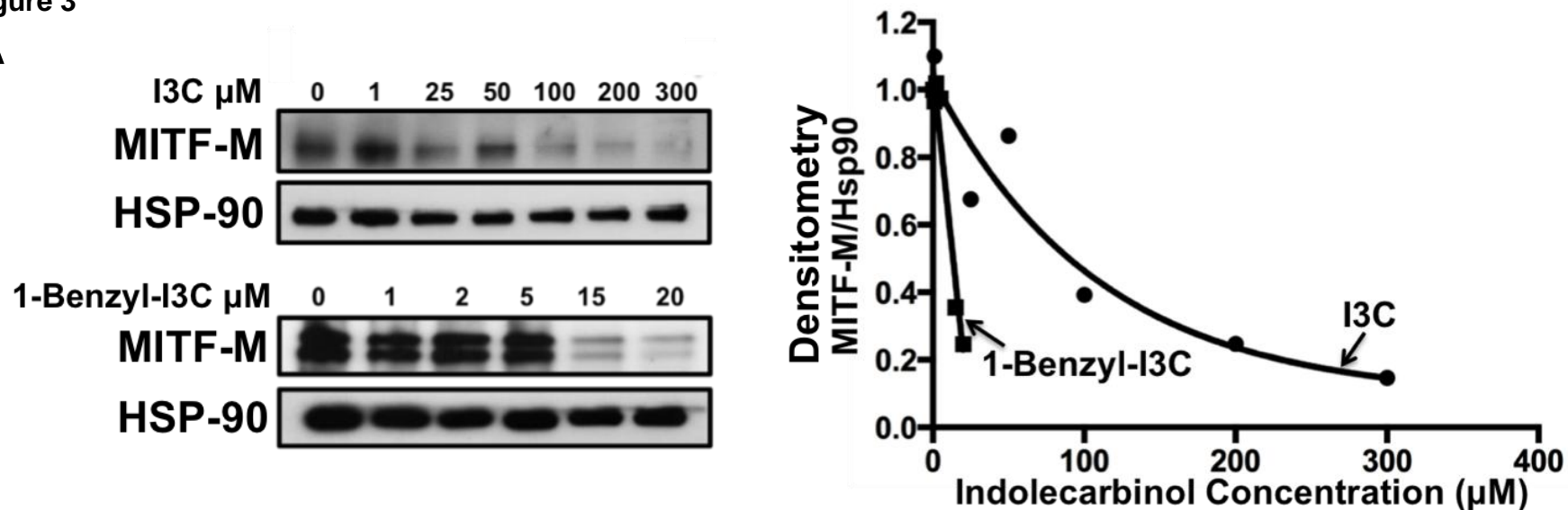


Figure 3

A



B

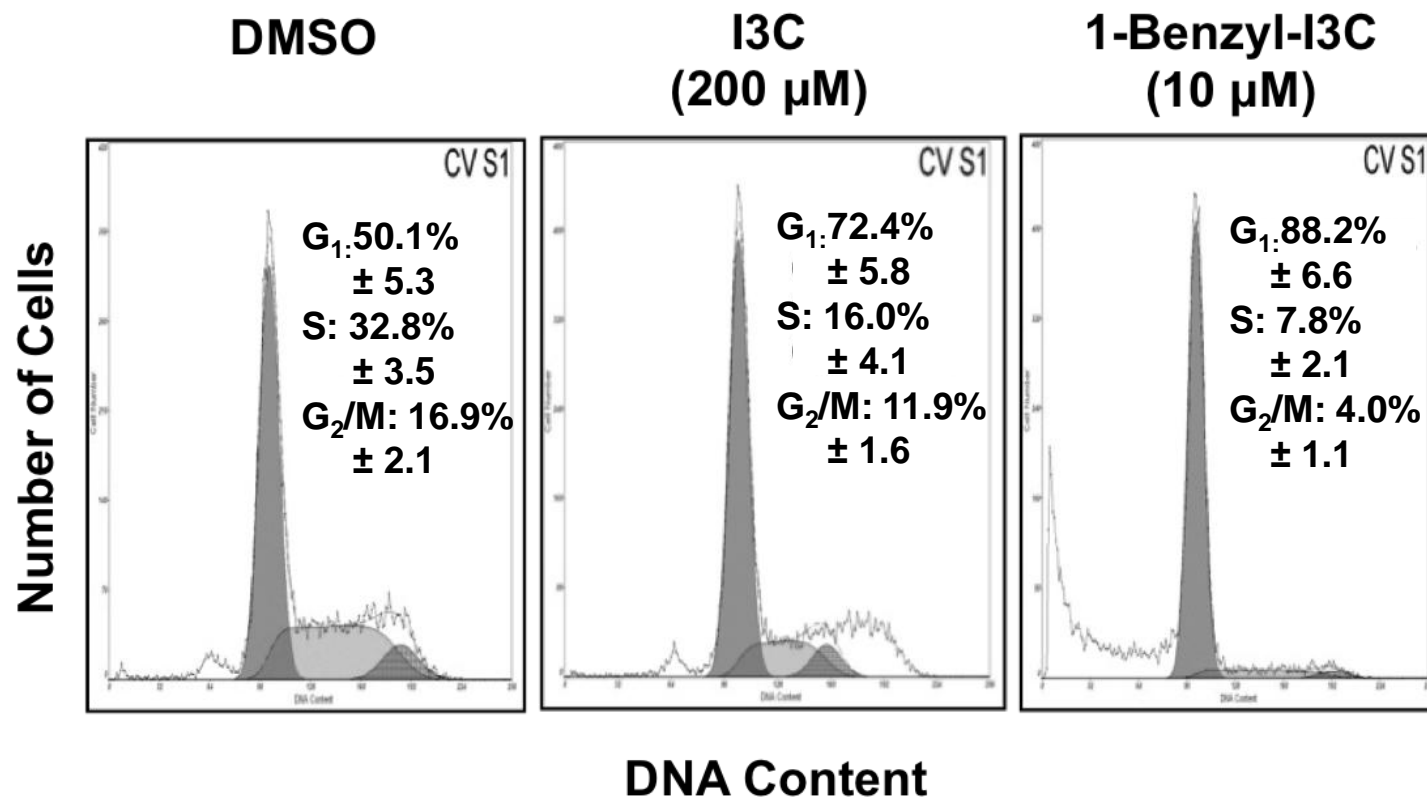


Figure 4

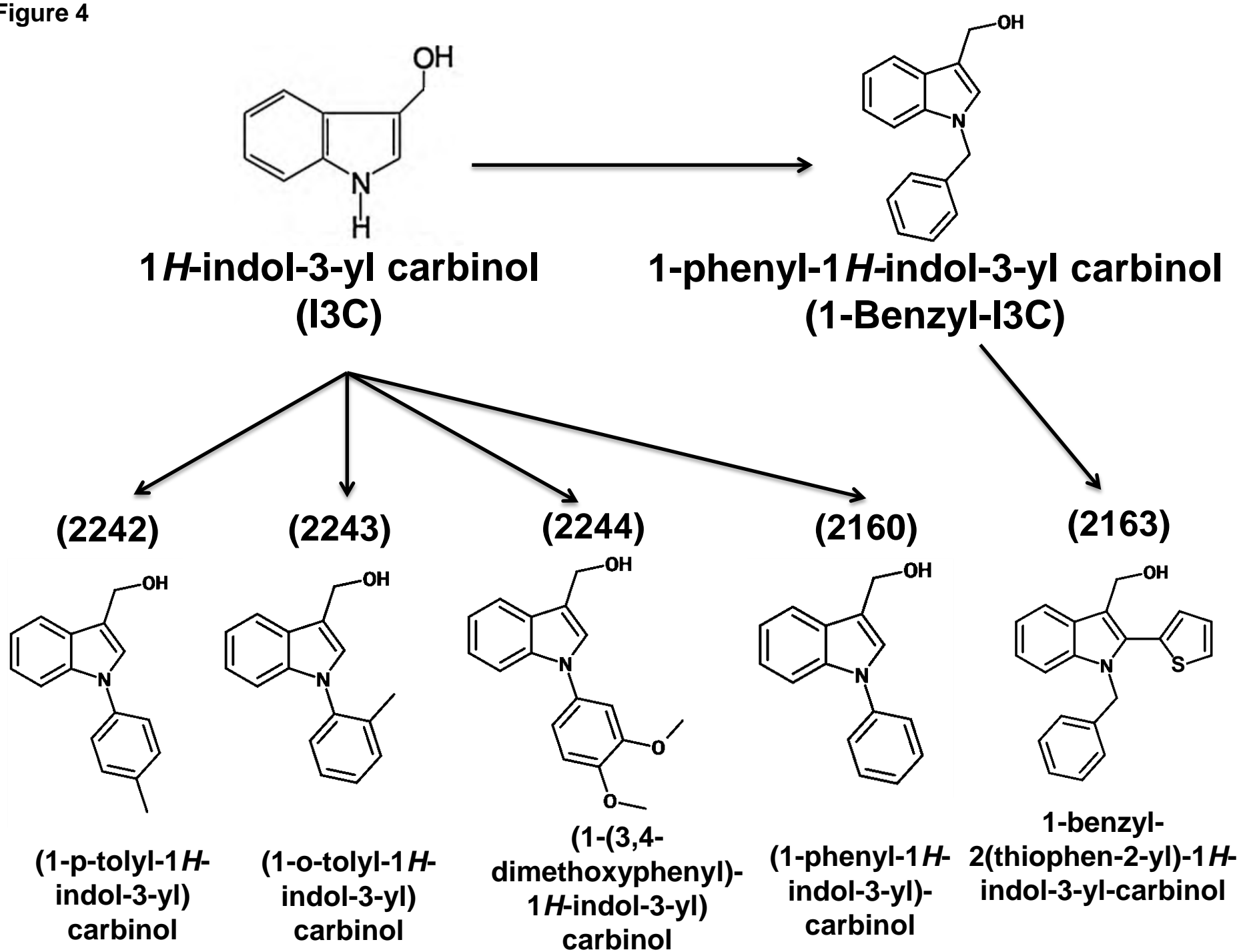


Figure 5

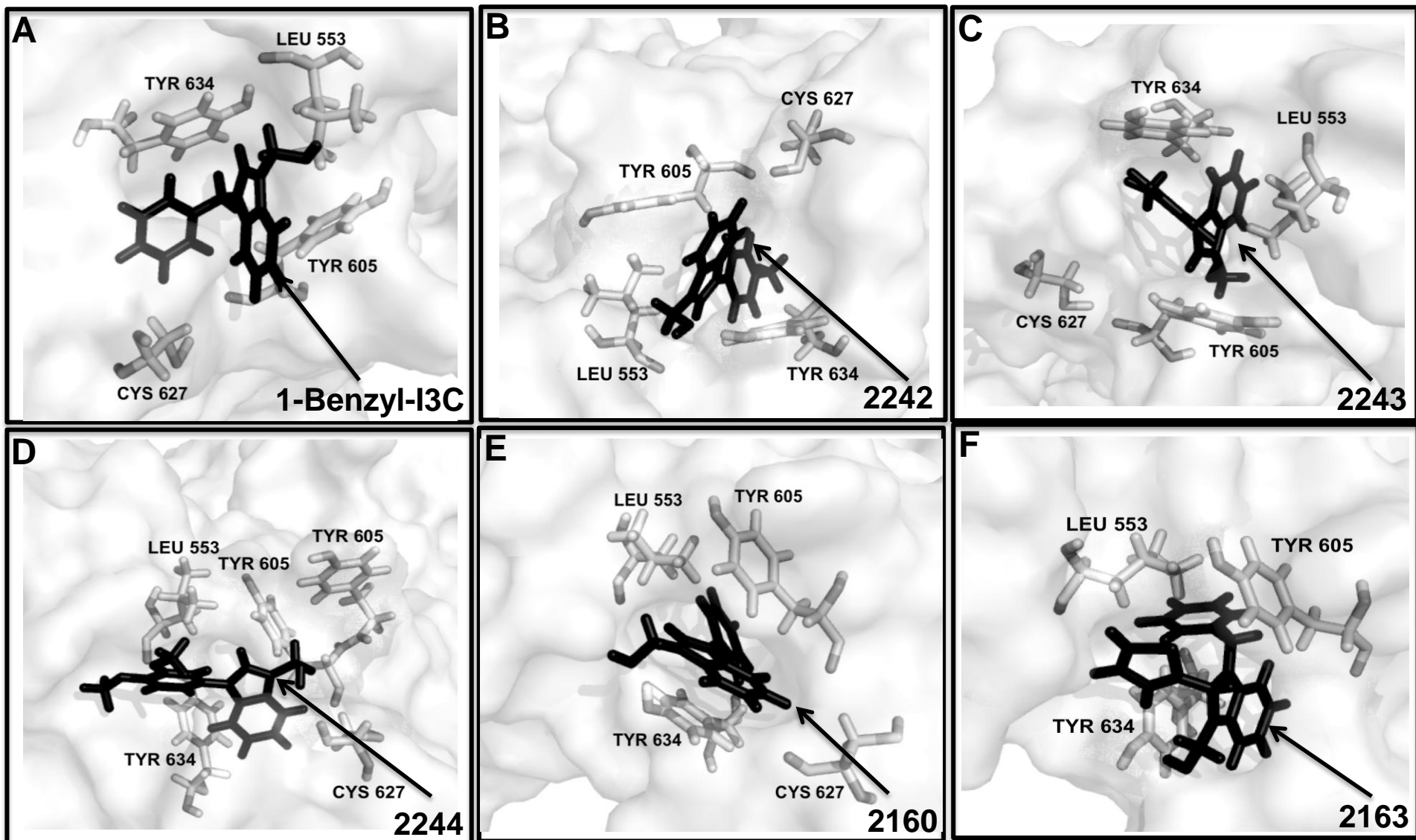
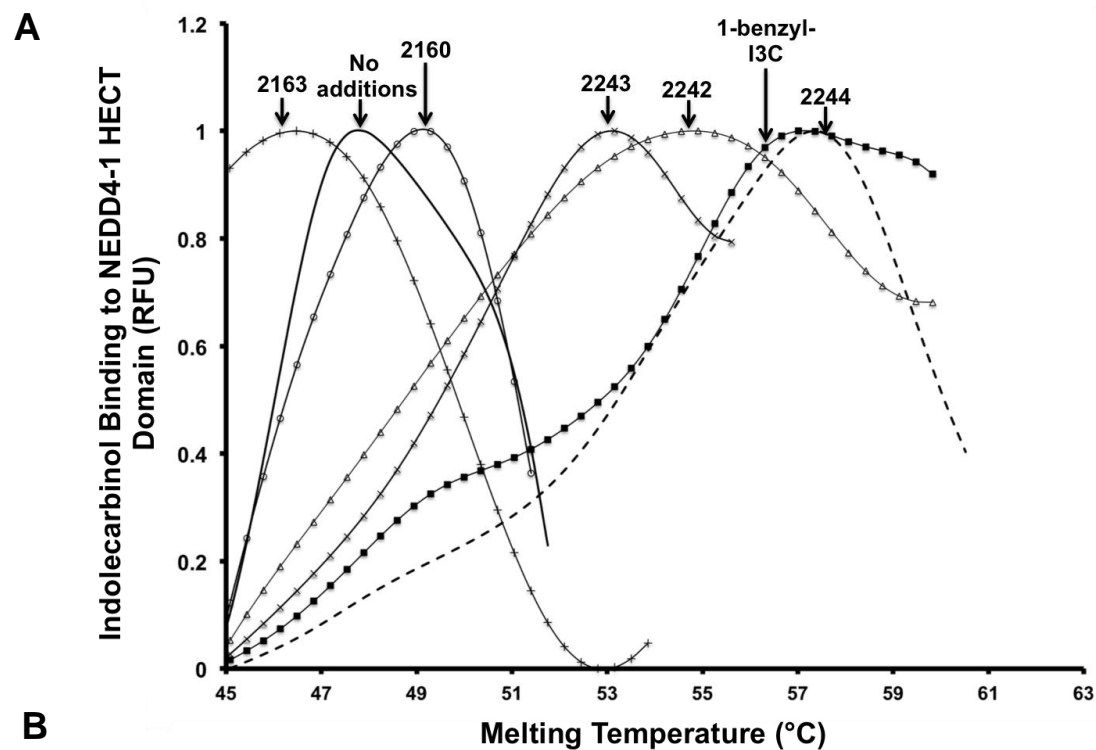


Figure 6



B

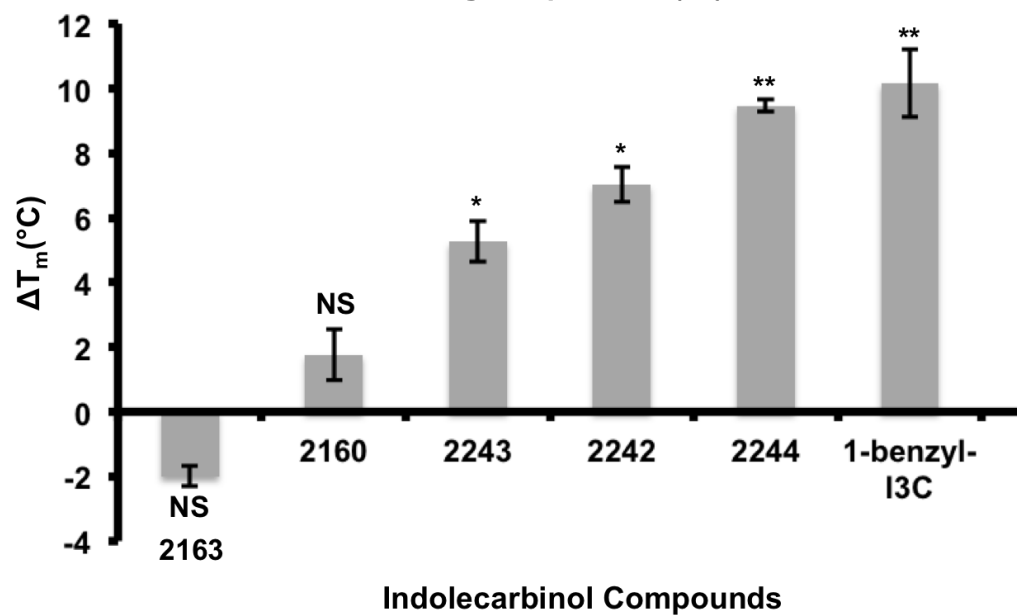


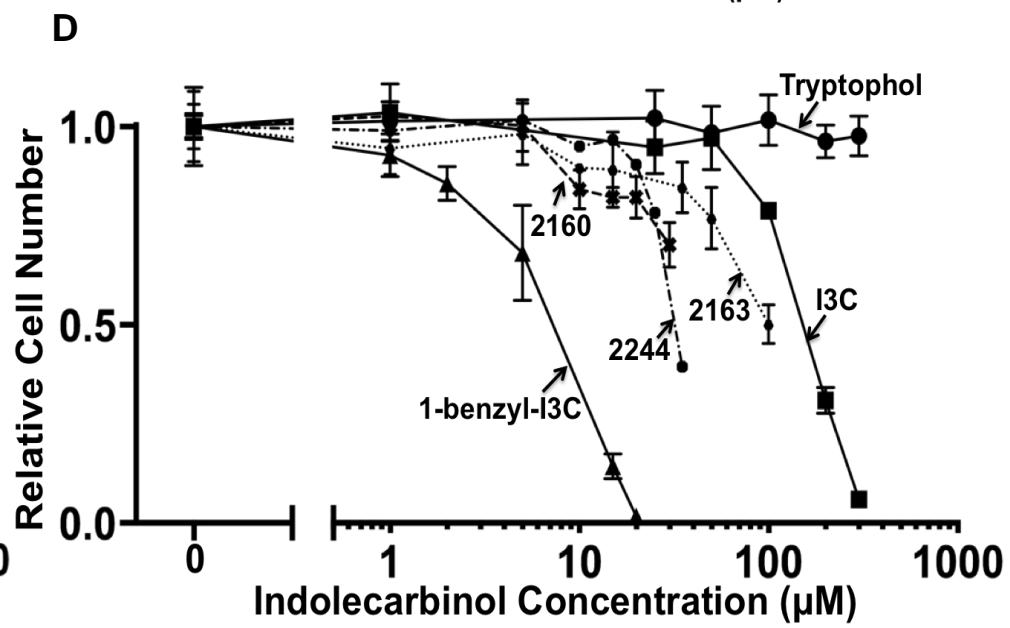
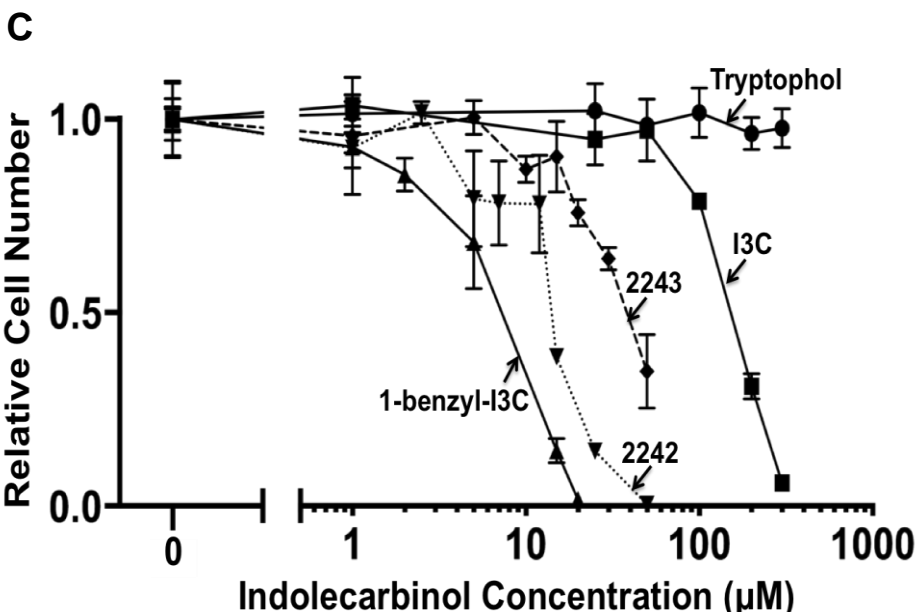
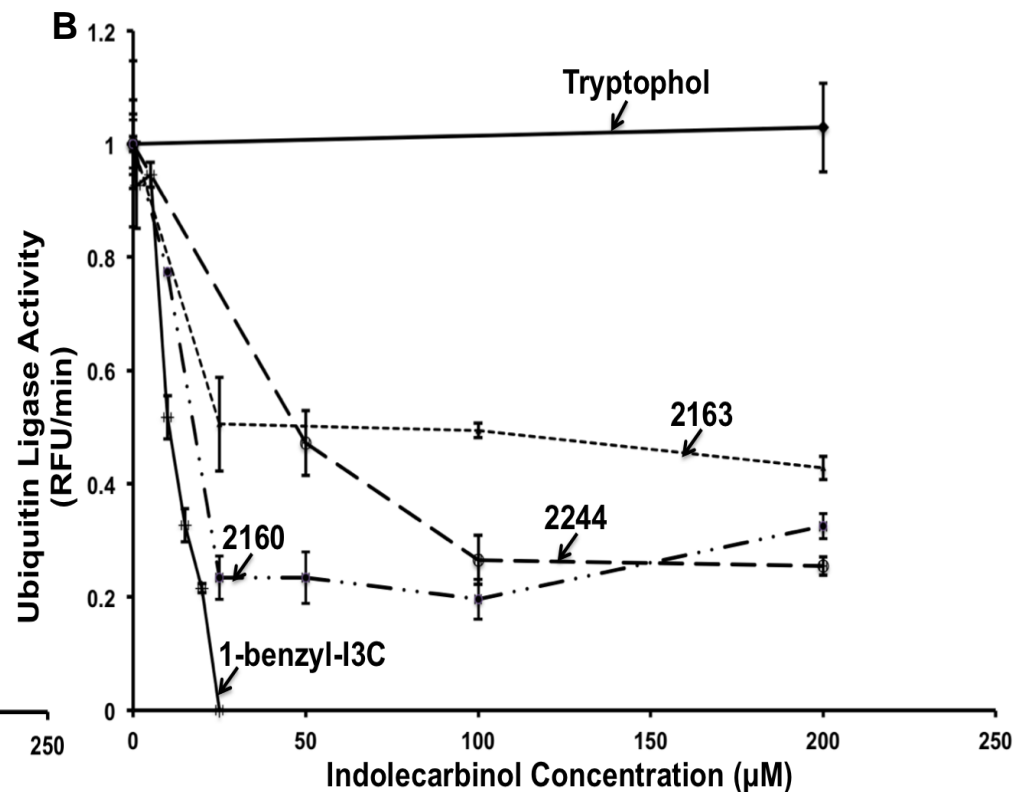
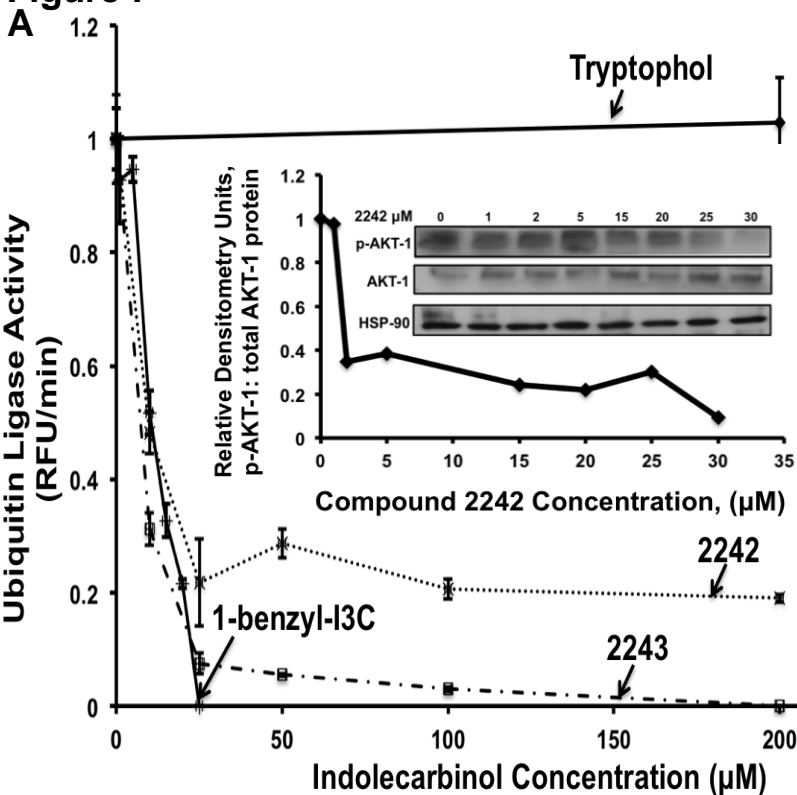
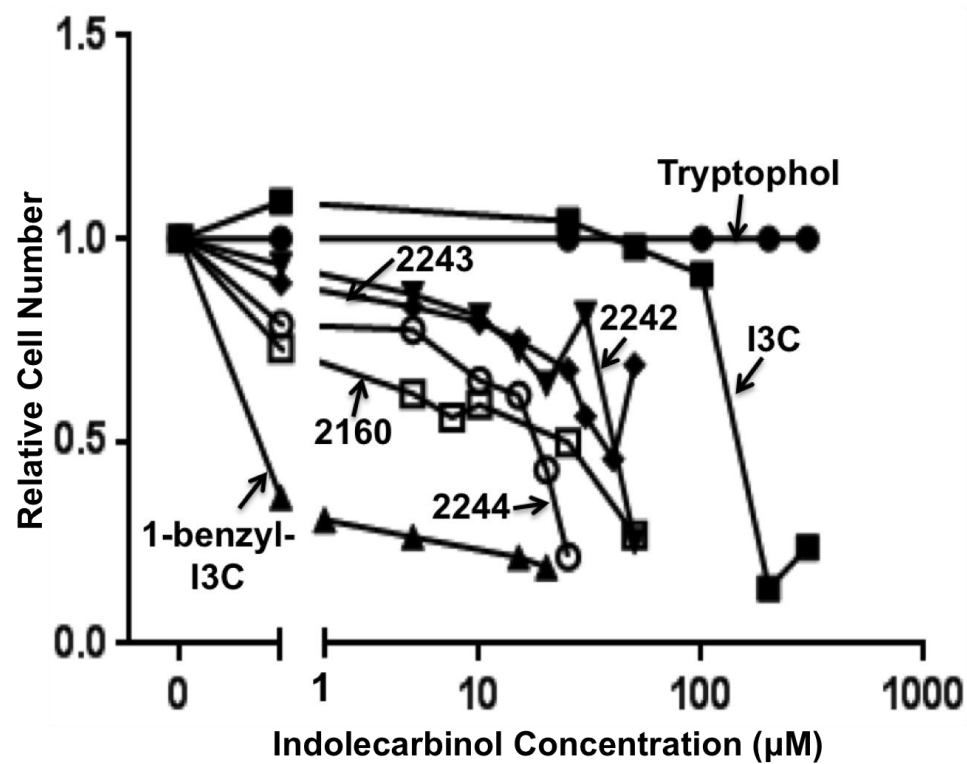
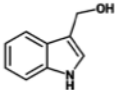
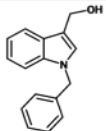
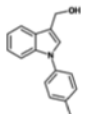
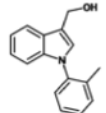
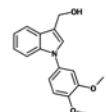
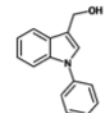
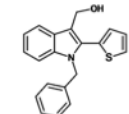
Figure 7

Figure 8

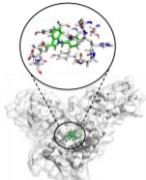


Indolecarbinol Compound	Half Maximum Concentration For Growth Inhibition in MCF-7 Cells (μM)
I3C	157.32
1-benzyl-I3C	0.87
2242	72.49
2243	58.44
2244	32.10
2160	40.83

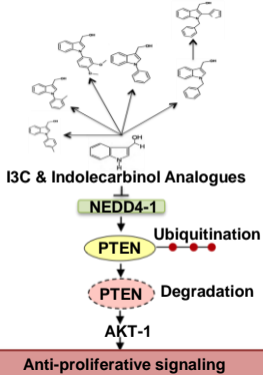
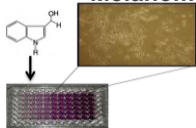
Figure 9

Indolecarbinol Compound	Structure	Half Maximum Inhibitory Concentration for NEDD4-1 Enzymatic Activity (μM)	Half Maximum Concentration for Growth Inhibition in G361 Cells (μM)
I3C		284	107
1-benzyl-I3C		12.3	14.7
2242		13	18.3
2243		7.9	25.1
2244		55.3	40
2160		32.4	47.1
2163		153	106

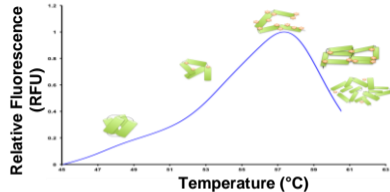
Molecular Docking



Anti-proliferative Effects in Human Melanoma Cells



Indolecarbinol Binding to NEDD4-1^{HECT}



Inhibition of NEDD4-1 Enzymatic Activity

